Preliminary Design: “The Hopper”

For Dr. Peter Gustafson

AAE 4690 Aircraft Design

Group 3

Brian Omondi Asimba

Adam Houtman

Jacob Maynard

Spring 2013

Abstract

A conceptual aircraft design is to be refined. These refinements will include stability, CG, performance, weight, internal arrangements, as well as arrangements of exterior surfaces such as windows, doors, access panels, etc. During this process, the wing was moved as were the engine nacelles and consequently the main landing gear. The overall wing span was slightly reduced and the chords were slightly increased. The horizontal tail saw an increase in area as well as a move slightly further aft. The vertical tail surface saw very small adjustments mostly as a result of the modeling it to the appropriate scale. Note that yaw stability analysis was unsuccessful as the code failed to yield accurate results. Therefore, the vertical tail dimensions did not get a chance to be adjusted if they need to be. The final design remains a traditional, twin, turboprop transport aircraft.

Contents

Aircraft Requirements

Aircraft is to be a regional airliner meeting the following specifications:

- Flight crew + 2 attendants
- 35 passengers (80kg+20kg per person)
- Associated baggage for crew, attendants, and passengers
- 800NM range
- Takeoff and landing with obstacle clearance at SSA (1000m)
- Design to FAR Part 25
- Light-weight materials is encouraged
- Use existing engines
- Customer may add additional requirements; design must have growth potential

Since profitability is a key requirement for this design, some market studying must be done to determine what other design requirements are implied with this stipulation. Aspects to determine what aircraft are the most profitable and/or most successful will include number of airframes built, time in service and number of variants as actual finances of a particular airline can be hard to acquire. With these determinants found, the following aircraft were found to be prime examples of an aircraft that operates in a similar category as the design to be made:

- SAAB 340
- Beech 1900D
- Embraer EMB 120 Brasilia
- Bombardier Dash 8 Q-series
- BAe Jetstream 41

These aircraft represent some of the most popular regional aircraft in service as well as a range of conventional designs. The BAe Jetstream has the lowest production run of ~100 units with the Dash 8 and Beech 1900 taking 1st and 2nd in production quantity. Note that the Dash 8 series shows the most growth potential as it has a wide variety of payload capability (number of passengers) as well as the largest production run of the aircraft presented here. Note that these will be explained in greater detail later.

Therefore, additional requirements for profitable operation were determined to be:

- Simple design-lower development cost
- Simple construction-ease of maintenance
- Easy access to systems
- Structure commonality

FAR 25 Requirements

Fuselage Considerations

While the above calculations provide a method to approximate the fuselage length and diameter, other requirements such as emergency exits and aisle sizing will ultimately determine the overall geometry. Other considerations are not made in this conceptual design, but will be examined for the preliminary design, such as fire safety equipment and structural limits.

Emergency Exits

FAR25.807 says that there must be at least two exits per side of the fuselage and that at least one on each side be a Type II door. A Type II door is 20" wide and 44" tall with a corner radius of no less than 10". The size of this door must be made a consideration when the fuselage diameter is chosen. The last requirement is that the two doors on either side of the fuselage must be at no more than 60ft apart.

Seating

FAR25.815 requires that the aisle be at least 20" wide to allow for quick departure of the aircraft in an emergency situation. This number has been found to the minimum needed for passengers to safely find emergency exits in a timely manner.

FAR25.817 states that for a single aisle aircraft, no more than three seats can be on either side of the aisle. This is to ensure that the passenger furthest from the aisle has enough time to get to an emergency exit in the event of an emergency.

Takeoff Requirements

Different speeds are required to be reached during the takeoff process. These are laid out in FAR25.107. The stall speed must be greater than the minimum ground control speed with one engine out (OEI), which cannot be calculated at this time. The final takeoff speed must be greater than 1.18 times the design stall speed. This takeoff data is required to be tested on smooth, dry, hard surface runways as this will provide the greatest friction for the tires in a typical takeoff.

The takeoff path is described in FAR25.111 and FAR25.113. The total takeoff distance is equal to 115% of the distance covered from brakes off to clearance of the obstacle with all engines operative. The climb gradient during the transition phase of takeoff must remain above 1.2% with gear down and flaps extended or above 3% if the gear and flaps are retracted.

Landing Requirements

FAR25.125 states that the aircraft must maintain an approach speed of at least 1.23 times the stall speed and a descent rate of at least 3.2%. It also states that the landing ground distance must be calculated assuming that all slowing devices are not functional, such as thrust reversers and air brakes.

Propeller Clearance

According FAR 25.925 the propeller disc has a proximity limit with respect to both the ground and the fuselage. For a tricycle gear aircraft, the propeller must be at least seven inches clear of the ground when the aircraft is fully loaded. The propeller disk must also maintain at least a one inch clearance of the fuselage.

Conceptual Review

In the conceptual design portion of this project, analysis was completed up to and including refined sizing. The results from this analysis are shown directly below in order to provide a reference starting point.

Table 1: Initial Weight Analysis Results

Initial Weight Approximation Method Results						
MTOW [lb]	Fuel [lb]	Empty Weight [lb]	Empty Fraction	Fuel Fraction	Max L/D Cruise	Max L/D Loiter
31243	6344	17877	0.572	0.203	17.87	15.48

Table 2: Power Loading and Wing Loading

Wing Loading/Power Loading Results						
P/W takeoff [hp/lb]	T/W takeoff	W/S Takeoff OEI [lb/ft^2]	T/W climb	Clmax	W/S stall [lb/ft^2]	W/S landing [lb/ft^2]
0.193	0.2	53.98	0.121	2.14	42.32	70.71
		W/S Takeoff [lb/ft^2]	T/W cruise	CLTO	W/S cruise [lb/ft^2]	
		107.95	0.089	1.77	129.74	

Table 3: Refined Sizing Results

Refined Weight Approximation Method Results						
MTOW [lb]	Fuel [lb]	Empty Weight [lb]	Empty Fraction	Fuel Fraction	P/W [hp/lb]	W/S [lb/ft^2]
29778	4860	17527	0.589	0.163	0.201	42.32

Wing and fuselage geometry, as well as tail sizing was also conducted within the conceptual design. Those results are not included here as the calculations were done outside of the computer code. This sizing has since been added to the code and will be considered the starting point of the preliminary design.

As a brief reminder of the overall configuration decided upon, a basic description of the Dash-1 model is given. Sonata is a traditional low wing, transport aircraft. Twin turboprop engines were selected due to the short range nature of the mission required. With a cruising speed of 210kts, the turboprop is more fuel efficient than the turbofan or turbojet. The selected engine is the PW127G, which provides about 5% more power required by the power loading analysis. The critical dimensions of the aircraft can be seen in the table below.

Table 4: Conceptual Dimensions (Dash-1)

W/S [lb/ft^2]	W0 [lb]	Sref [ft^2]	AR	ΛLE	Λc/4	λ
42.32	29778	704	11	10	8	0.614
b [ft]	**Cr [ft]**	**Ct [ft]**	**c bar [ft]**	**x_fuse [ft]**	**y bar [ft]**	**x bar [ft]**
88	9.9	6.1	8.15	81	20.2	5.61

The main wing is a standard rectangular wing with winglets, with a small taper on both the leading and trailing edges. The wing is equipped with flaps, slats, and slats, as well as de-icing equipment. The horizontal tail is also rectangular with no sweep, and a small taper. The vertical stabilizer is swept back about 30 degrees, with ventral strakes on the bottom of the fuselage set at 45 degrees off vertical. The gear is arranged in a tricycle configuration with the main gear located in the nacelles of the engines. The wing is positioned at about the midpoint of the fuselage.

Equations and procedure to be used in analysis

Wing/Fuselage Sizing

The fuselage length is found initially from an empirical equation provided by Raymer in chapter 6. The equation is based off of the predicted maximum takeoff weight and two historically-based coefficients.

$$Length = aW_0{}^C \qquad (Table\ 6.3)$$

For a twin turboprop, ‘a’ and ‘c’ are .37 and .51, respectively. This length of 71ft is used as a starting point and is then either extended or reduced to accommodate the necessary number or passengers, as well as baggage space, APU space, and other equipment. The diameter of the

fuselage is driven by the needed interior height and width for passenger loading. Another factor in determining the fuselage diameter is the fineness ratio, a measure of "sleekness" or aerodynamic cleanliness. Raymer suggests that for a fixed volume, subsonic aircraft, a fineness ratio between six and eight.

The wing geometry is then determined from geometrical relations between the wing area, desired aspect ratio, taper ratio, and sweep. The mean aerodynamic chord, '$\bar{c}$ ', is also found from the same geometrical constraints.

$$b = \sqrt{AR * S} \qquad Eq\ (7.5)$$

$$c_{root} = \frac{2S}{b(1+\lambda)} \qquad Eq\ (7.6)$$

$$c_{tip} = \lambda c_{root} \qquad Eq\ (7.7)$$

$$\bar{c} = \frac{2}{3} c_{root} \frac{1+\lambda+\lambda^2}{1+\lambda} \qquad Eq\ (7.8)$$

$$\bar{x} = \frac{1+2\lambda}{12} c_{root} AR \tan \Lambda_{LE} + .25\bar{c}$$

$$\bar{y} = \left(\frac{b}{2}\right) \frac{1+2\lambda}{3(1+\lambda)} \qquad Eq\ (7.9)$$

The wing reference area was found by dividing the maximum takeoff weight by the selected wing loading. Initial tail sizing was done using volume coefficients provided by Raymer in chapter 6. 'X' is the distance measured from the apex of the root chord to the apex of the MAC and 'X bar' is the distance from the apex of the root chord to the aerodynamic center of the MAC. The results of these calculations can be found in the table below.

Table 5: Wing/Tail Geometry

Span [ft]	Croot [ft]	Ctip [ft]	MAC [ft]	Y bar [ft]
99.6	10.3	6.3	8.5	22.9
X [ft]	X bar [ft]	VT Area [ft^2]	HT Area [ft^2]	
4	6.2	147.7	141.1	

Wetted Area Buildup

Now that the general geometry of the aircraft has been determined, the actual wetted area of the aircraft can be determined in order to validate the early lift and drag characteristics. In chapter 7, Raymer lays out equations for approximating the wetted area of the wing, fuselage, tail surfaces, and nacelles. The fuselage equations are based off of the projected areas from the top and side views. The wings and tail surfaces are based on their respective exposed areas and thickness-to-chord ratios. The nacelles were approximated using the dimensions of the chosen engine.

$$S_{wet,wing} = S_{exposed}\left[1.977 + .52\left(t/c\right)\right] \qquad Eq\ (7.12)$$

$$S_{wet,fuse} \cong 3.4\left(\frac{A_{top} + A_{side}}{2}\right) \qquad Eq\ (7.13)$$

The results from these calculations can be seen in the table below with units of square feet.

Table 6: Wetted Area Buildup

Wing	VT	HT	Fuselage	Nacelles
1358	300	286	1897	140

The areas are summed for a total of 3981ft^2, resulting in a new wetted area ratio of 4.82, lower than the original prediction.

Weight Breakdown

In order to obtain an accurate balance of the aircraft for stability, the location and weight of each individual component needs to be known. Raymer provides equations for 21 of the most essential components in a commercial aircraft. Several of these components can be further broken down, but that is beyond the scope of this project. The equations and variables for these will not be listed here to preserve the length of this report, but both can be found in chapter 15 of Raymer's text, specifically equations 15.25 through 15.45. The location of each component is not provided and therefore requires placing by the design team. The sum of all of the components must be equal to or below the empty weight, or else weight must be deducted elsewhere, meaning less fuel or less passengers.

The results of these calculations can be seen in the table below.

Table 7: First Weights Breakdown

Component	Weight [lb]	Component	Weight [lb]
Wing	3249	Flight Controls	924
HT	191	APU	524
VT	279	Instruments	208
Fuselage	4482	Hydraulics	255
Main Gear	1321	Electrical	792
Nose Gear	508	Avionics	1235
Nacelles	734	Furnishings	642
Engine Controls	42	A/C	504
Starter	74	Anti-Ice	60
Fuel System	225	Engines	2128
Passenger Seats	1184	Pilot Seats	120

This gives a total empty weight of 19718lb, 3235lb overweight. Since both passenger count and range are requirements for the design, neither payload weight nor fuel weight can be reduced. This prompts a reanalysis of the sizing method, utilizing the new heavier empty weight.

Reanalyzing the Weight

The refined sizing method code is altered such that the new empty weight is added to the previously used passenger, fuel, and crew weights to find a new total weight. This new weight is then divided by the original prediction, raised to the .9 power, and then multiplied by the heavier empty weight. The result is an even heavier empty weight, now accounting for the added structure needed to compensate for the higher MTOW. This method is described by Raymer in chapter 19 in greater detail.

A new prediction is made for the takeoff weight, and the refined sizing method is again iterated until convergence. Wing loading and thrust loading are also rechecked to ensure that the new heavier design is still capable of the necessary performance as specified by the customer.

Table 8: Second Refined Sizing Results

MTOW [lb]	Fuel [lb]	Empty Weight [lb]	Empty Fraction	Fuel Fraction	P/W [hp/lb]	W/S [lb/ft^2]
34202	5063	21749	0.636	0.148	0.172	34.02

The new weight is substantially heavier than the earlier predictions. However, it is not uncommon for aircraft to “gain weight” as the design process progresses, and this design is still

competitive with the benchmarked aircraft. The wing loading has decreased suggesting a larger wing is now necessary to maintain the takeoff requirements. The power loading change further reinforces the decision to go with a more powerful engine.

Redesigned Geometry and Wetted Area

Since the weight, wing loading, and power loading have all changed, the geometry and initial sizing needs to be repeated. The methods for this won't be repeated here and the results can be seen in the table below.

Table 9: Second Sizing Results

Span [ft]	C_{root} [ft]	C_{tip} [ft]	MAC [ft]	Y bar [ft]
100.3	12.4	7.6	10.2	23.1
X [ft]	**X bar [ft]**	**VT Area [ft^2]**	**HT Area [ft^2]**	
5.4	7.9	166.1	190.4	

The overall size of the wing has increased and the taper ratio was also decreased in order to maintain the desired aspect ratio. The fuselage length increased to 76ft, which is still shorter than what is needed in order to host 35 passengers, baggage, and other equipment. The general increase in size demands that the wetted area ratio is again reexamined.

Table 10: Second Wetted Area Buildup

Wing [ft^2]	VT [ft^2]	HT [ft^2]	Fuselage [ft^2]	Nacelles [ft^2]
1653	337	386	1897	140

The new total wetted area is 4413ft^2 and provides a new wetted area ratio of 4.39. Although the aircraft has increased drastically in weight, the aerodynamics have been retained. This is most likely attributed to the frozen fuselage and engine size as the wing increased in size.

Refined Weight Breakdown

Now that the new geometry has been set, the same weight breakdown of the key components can be completed. The second time around, the empty weight total ends up being a few hundred pounds lighter than what is predicted, allowing for the possibility of carrying additional passengers or increasing the fuel capacity. The final locations are also displayed here, relative to the nose of the aircraft, but are explained in greater detail in the internal arrangement section.

Table 11: Final Weight Breakdown

Component	Weight [lb]	Location [ft]	Component	Weight [lb]	Location [ft]
Wing	4119	35.3	Flight Controls	924	38.9
HT	263	81	APU	524	70
VT	342	83.2	Instruments	212	9.5
Fuselage	4965	38	Hydraulics	264	42
Main Gear	1573	41.5	Electrical	792	38
Nose Gear	577	10.4	Avionics	1235	7
Nacelles	734	29.2	Furnishings	642	19.8
Engine Controls	42	29.2	A/C	504	55
Starter	74	29.2	Anti-Ice	73	40
Fuel System	225	37.9	Engines	2128	29.2
Passenger Seats	1184	40	Pilot Seats	120	13.3
Lavatory	35	60			

Aerodynamics

With the configuration and size of the aircraft now set, aerodynamic studies can be completed. The key parameter investigated here is zero-lift drag in two different configurations, cruise and takeoff. Chapter 12 of Raymer's text describes two methods for approximating the 'C_{D0}'. The method selected for use here is the component buildup method. The major components of the aircraft, such as the tail surfaces, wing, fuselage, and engines are examined for both conditions, with the addition of landing gear drag for takeoff.

The first step for this is to find the local Reynold's number of each major component. This will vary since Reynold's number is dependent on the length of the object that the air is passing over. The mean chord will be used for the wing and tail surfaces, while the fuselage and nacelles will use their full length.

$$Re = \frac{\rho v l}{\mu} \qquad Eq\ (12.25)$$

Where' ρ' is the air density,' v' is velocity, l is length, and 'μ' is the dynamic viscosity of air, with 'ρ' and 'μ' varying with altitude. A friction coefficient is then determined for each component. This coefficient is determined from a weighted average of the laminar and turbulent coefficients. The weight of laminar versus turbulent flow is dependent on the shape of the object in question. Raymer suggests that for a fuselage or nacelle that the flow is 90% turbulent and for a wing that the flow is 65% turbulent.

$$C_{f_{lam}} = 1.328/\sqrt{Re} \qquad Eq\ (12.26)$$

$$C_{f_{tur}} = \frac{.455}{(log_{10}Re)^{2.58}} \qquad Eq\ (12.27)$$

Form factors are then found to account for the slight pressure drag effects.

$$FF_{wing} = \left[1 + \frac{.6}{(x/c)_m}\left(\frac{t}{c}\right) + 100\left(\frac{t}{c}\right)^4\right][1.34M^{.18}(\cos\Lambda_m)^{.28}] \qquad Eq\ (12.30)$$

$$FF_{fuselage} = \left(1 + \frac{60}{f^3} + \frac{f}{400}\right) \qquad Eq\ (12.31)$$

$$FF_{nacelle} = 1 + (.35/f) \qquad Eq\ (12.32)$$

where $(x/c)_m$ is .3 for low speed airfoils, t/c is the thickness to chord length ratio, and f is the length over diameter. Lastly, interaction effects, 'Q', between the components must be accounted for, as these increases the drag. Raymer provides values for these, 1.5 for the nacelles, 1.1 for the wing, and 1.04 for the tail surfaces. Each component's contribution to the total drag is found from the following equation.

$$C_{D0_{comp}} = C_f * FF * Q$$

Other factors of the aircraft's design add drag, with the most significant being the upsweep at the rear of the fuselage. For takeoff, the drag created by the landing gear is approximated using an empirical table provided by Raymer. The frontal area of the wheel, linkages, and hydraulic systems determine the amount of the drag contributed.

Table 12: Zero-Lift Drag

Cruise C_{D0}	Takeoff C_{D0}
0.023	0.048

The drastic difference in drag is exactly why retractable gear are well worth the added weight. It more than doubles the drag.

Center of Gravity

The placement of the center of gravity within the aircraft is paramount in ensuring that the aircraft is stable. The center of gravity can be controlled by the designer by moving key components to different locations of the aircraft, such as can be seen by APUs being often located in the tail of aircraft. For an initial estimate of where the CG should be, the quarter-

chord of the main wing is used as a goal. Four different flight conditions are analyzed for four different CGs; empty, fuel only, passengers only, and MTOW.

The final location of the CG in each condition is shown below. These results were reached after over 100 iterations of fine tuning the size and locations of the components in order to satisfy the longitudinal stability criteria, explained in the next section. The MAC is located about 39ft.

Table 13: CG Locations

Empty [ft]	Fuel Only [ft]	Passengers Only [ft]	MTOW [ft]
35.7	36.4	37.7	37.9

These results suggest that the aircraft becomes more stable and less maneuverable as fuel is burned. Since it is a passenger transport, maneuverability is not a major concern, whereas a stable aircraft is. The more stable the aircraft, the less experienced the pilot needs to be, although a more experienced pilot is always suggested.

Longitudinal Stability

Longitudinal stability describes the aircraft's ability to correct perturbations affecting the pitching moment of the aircraft. The aircraft must maintain this stability throughout the flight. This is determined by the static margin, a measure of the distance between the CG and the neutral point. The neutral point is the aft most CG allowable for the aircraft to maintain stability. The design should also require that the aircraft require as little elevator input as possible to reduce trim drag. This optimization determines the forward most location of the CG allowable.

Longitudinal stability needs to be determined for three phases of flight; cruise, approach, and takeoff. The most important equations for finding the neutral point are shown below, with several others available for further investigation in chapter 16 of Raymer's text. The neutral point is found for each phase of flight and displayed as the static margin in the table.

$$\bar{X}_{np} = \frac{C_{L_\alpha}\bar{X}_{acw} - C_{m_{\alpha fus}} + \eta_h \frac{S_h}{S_w} C_{L_{\alpha_h}} \frac{\partial \alpha_h}{\partial \alpha} \bar{X}_{ach} + \frac{F_{P_\alpha}}{qS_w}\frac{\partial \alpha_h}{\partial \alpha}\bar{X}_P}{C_{L_\alpha} + \eta_h \frac{S_h}{S_w} C_{L_{\alpha_h}} \frac{\partial \alpha_h}{\partial \alpha} + \frac{F_{P_\alpha}}{qS_w}} \qquad Eq\ (16.9)$$

$$C_{m_{cg}} = C_L\left(\bar{X}_{cg} - \bar{X}_{acw}\right) + C_{m_w} + C_{m_{w\delta f}}\delta_f + C_{m_{fus}} - \eta_h \frac{S_h}{S_w} C_{L_h}\left(\bar{X}_{ach} - \bar{X}_{cg}\right)$$

$$-\frac{T}{qS_w}\bar{Z}_t + \frac{F_P}{qS_w}\left(\bar{X}_{cg} - \bar{X}_P\right) \qquad Eq\ (16.7)$$

To find the necessary elevator input for proper trim, 'C_{mcg}' must equal zero. The elevator deflection angle influence on the equation is found in 'C_{Lh}', as an input in finding '$\Delta\alpha_{0L}$'.

$$\Delta\alpha_{0L} = \left(-\frac{1}{C_{L_\alpha}}\frac{\partial C_l}{\partial \delta_e}\right)\delta_e \qquad Eq\ (16.16)$$

This change in zero-lift angle of attack is added to the angle of attack that the horizontal tail is already seeing.

$$C_{L_h} = C_{L_{\alpha h}}(\alpha + i_h - \epsilon - \alpha_{0Lh} + \Delta\alpha_{0Lh}) \qquad Eq\ (16.14)$$

The remaining coefficients and variables can be found explained in chapter 16 of Raymer's text. Initial calculations for static stability showed that the aircraft was just stable enough in cruise, but unstable in approach. A large amount of shifting of the wing, engines, and APU was done to provide a stable aircraft in all three flight phases.

The trim calculations were then completed, showing that the aircraft needed zero trim when flying straight and level. However, this came at a cost of needing nearly 10 degrees of elevator deflection to overcome one degree of pitch. This meant that the aircraft would not be able to correct itself in the presence of a large gust or pilot error. A large amount of shifting of the wing, as well as resizing the tail and elevator could not overcome this problem. Ultimately, the entire interior layout had to be rearranged allowing for a more forward CG. This also required shifting the wing and engines further forward to further move the CG. Eventually, a long enough moment arm was obtained for adequate control. The static stability was also considered adequate, despite the still low margin for approach. A fly-by-wire system should be able to account for this.

Table 14: Static Margins

Cruise			
Neutral Point (% MAC)	**MTOW SM (% MAC)**	**No Passengers SM (% MAC)**	**Empty Fuel (% MAC)**
37.3	7.4	22.8	9.3
Approach			
Neutral Point (% MAC)	**MTOW SM (% MAC)**	**No Passengers SM (% MAC)**	**Empty Fuel (% MAC)**
36.3	1.3	16.7	3.2
Takeoff			
Neutral Point (% MAC)	**MTOW SM (% MAC)**	**No Passengers SM (% MAC)**	
37.3	4.4	19.9	

Empty fuel conditions were analyzed for cruise and approach, but not takeoff. This is because a takeoff will never occur with no fuel and the aircraft becomes more stable as fuel is burned, meaning that if there is a low fuel takeoff, the static margin will be higher than the MTOW. For cruise, there is a chance that the aircraft could use all of its fuel and be forced to divert, so stability in this condition is important. Approach is done under the same assumptions as cruise.

No passenger was investigated due to ferry flights. All aircraft need to be tested with no passengers onboard as well as be able to fly from airport to airport empty. MTOW was investigated for all conditions, even though a true maximum weight will only be encountered during takeoff. In the event of an abandoned takeoff after the aircraft is in the air, the aircraft is still stable in the approach configuration.

Major differences for the takeoff conditions arise from the effect of landing gear. The friction between the tires and the ground creates a pitching moment, as well as the ground “pushing back” on the tires. Both approach and takeoff analysis is done with full flaps, while cruise has no flap deflection.

The trim plot below shows how the moment about the center of gravity is affected by the deflection of the elevator at differing angles of attack. Where the lines cross the x-axis (horizontal blue line) shows what elevator deflection is needed to fly level at that angle of attack. The line furthest to the left represents negative two degrees of elevator deflection, with each line to the right increasing by two degrees. The dots represent the angle of attack, with zero being furthest left and 10 degrees on the right. This graph shows that for no trim input, the aircraft must cruise at about 3.8 degrees of angle of attack. If the elevator deflects -2 degrees, only 2.1 degrees of alpha is needed for level flight.

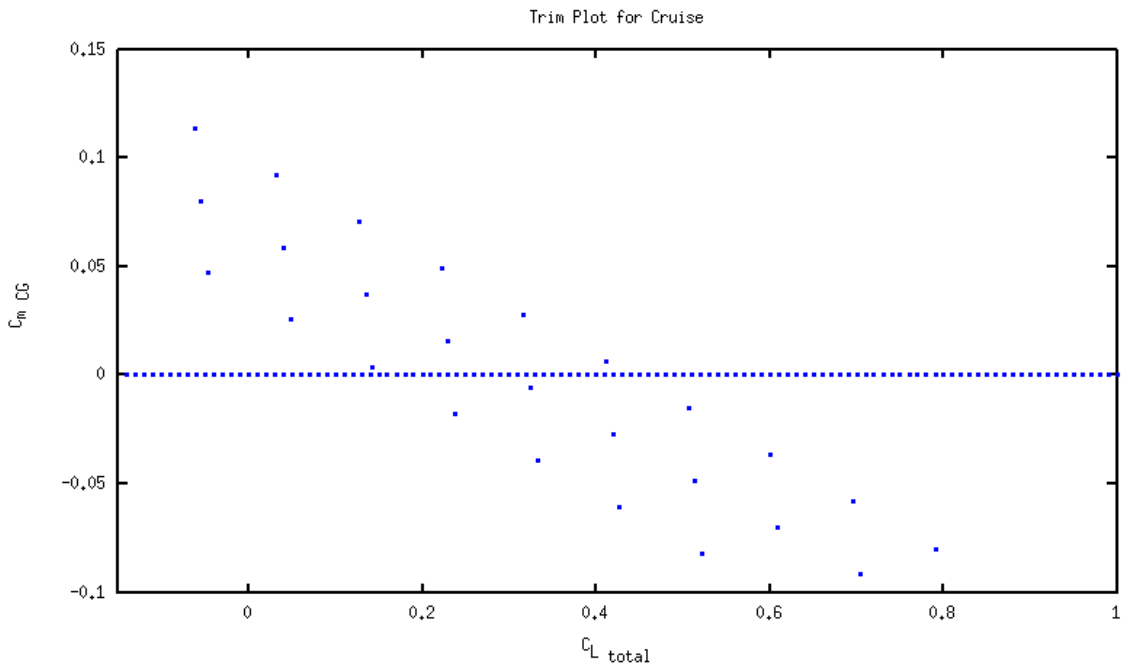

Figure 1: Trim Plot (Cruise)

Lateral Stability

Lateral stability is the aircrafts ability to correct itself when introduced to perturbations in the yaw and rolling axes. Roll and yaw are calculated together since the two are coupled moments. When the aircraft yaws, a roll is induced due to the differential drag on each wing. When the aircraft rolls, a yaw is created from the resultant force on the vertical tail.

Two conditions that are of the upmost importance are OEI takeoff and crosswind landing. For a crosswind landing, the FAA states that an aircraft must be able to land with a crosswind that is 20% of their forward velocity. This results in a yaw angle, 'β', of 11.5 degrees. For OEI, the rudder input must be able to overcome the sideslip induced by the asymmetric thrust and drag induced by the engines. Equation 16.38 shows how to find the yawing moment induced by OEI operation. Equation 16.40 is used for finding the rolling moment induced in either of the above mentioned flight conditions. For crosswind landing, the thrust and drag components are canceled (balanced forces) and the propeller wash effect is doubled. Each of the individual variables and constants can be further investigated by referring to chapter 16 of Raymer's text.

$$C_n = C_{n_{\beta_w}}\beta + C_{n_{\delta_a}}\delta_a + C_{n_{\beta_{fus}}}\beta + C_{n_{\beta_v}}\beta - \frac{T\bar{Y}_p}{qS_w} - \frac{D\bar{Y}_p}{qS_w} - \frac{F_P}{qS_w}\left(\bar{X}_{cg} - \bar{X}_p\right) \quad Eq\ (16.38)$$

$$C_l = C_{l_{\beta_w}}\beta + C_{l_{\delta_a}}\delta_a + C_{l_{\beta_v}}\beta \quad Eq\ (16.40)$$

Drag of the wind-milling propeller is found from chapter 12 of Raymer's text for a feathered propeller. Thrust is found from the thrust to weight ratio and is halved since one engine is not producing thrust.

Results from the code were not conclusive for lateral stability. The results suggested that the aircraft would have reduced sideslip if the engines were moved further outboard, which is known to be false. Unfortunately, there wasn't time available for the bug in the code to be found, as several other erroneous conclusions were being displayed. Therefore, lateral stability requires further investigation.

Tire Sizing

The term wheel is the circular metal/plastic object around which the rubbers "tire" is mounted. During landing, the brake system which is used to slow down the aircraft is mounted inside the wheel. Today, most tires are pneumatic inflatable which may include a doughnut shaped body of chords encased within. There are four important functions of the tire:

- They are used to support the aircraft structure off the ground.
- They help to absorb shock from the runway surface.
- They help in the transmission of acceleration and braking forces from the runway surface.
- They help in the steering of the airplane in different directions.

Tire sizing was first done by calculation of the diameter of the tires, which are the main as well as the nose wheel tire. From there, the tire width is calculated and the closest tire in the market that is closer in terms of the maximum static load was selected from the manufacturer's catalog. The tire selection was however based on the smallest diameter that was rated to carry the static and dynamic loads that were calculated.

The main tires were designed to carry 90% of the total aircraft weight while the nose wheel was designed to carry 10% of the total weight. The tire sizing process began with the calculation of the diameter and width of both the nose tires as well as the main tires. In order to do this, the equation given in table 11.1 from Raymer's textbook was used, which was given by:

$$d = AW^B$$

From there the width of the main wheel was calculated using the equation given by:

$$w = AW^B$$

In both of these equations W is 90% of the total take off gross weight.

Both A and B values were determined and from there the diameters and the width of the wheels were calculated. The same was done for the nose gear but only 10% of the total weight was used in the calculations. Table 1 shows the results from the calculations.

Table 15: Tire Width/Diameter

	Main Gear	Nose Gear
Tire Diameter(in.)	27	16.8
Tire Width(in.)	7.5	3.6

Next, the maximum and minimum static and dynamic loads and the total loads were determined by use of Raymer's equations 11.1 to 11.4 which are given by:

$$(Max\ Static\ Loads) = W\frac{N_a}{B} \qquad Eq\ (11.1)$$

$$(Max\ Static\ Loads)_{nose} = W\frac{M_f}{B} \qquad Eq\ (11.2)$$

$$(Min\ Static\ Loads)_{nose} = W\frac{M_a}{B} \qquad Eq\ (11.3)$$

$$(Dynamic\ Braking\ Load)_{nose} = \frac{10HW}{gB} \qquad Eq\ (11.4)$$

Where:
W-Maximum Takeoff Weight
N_a-Distance between the Nose Wheel and the aft Center of Gravity
N_f -Distance between the Nose Wheel and the forward Center of Gravity
M_a-Distance between the Main Wheel and the aft Center of Gravity
M_f-Distance between the Main Wheel and the forward Center of Gravity
H-Distance from the aircraft cg to the ground

The distance for the main gear H, was determined by addition of the FAR 25 propeller distance to the radius of the propeller. The requirement of more than seven inches since we were using a nose wheel landing gear.

$$H = H_{clr} + \frac{D_P}{2}$$

Where:
H_{clr}-Propeller clearance

The propeller diameter which was determined as 13.4 ft was used. The distance H was found to be 7.5ft.

Since this aircraft is operating under FAR 25, a 7% margin was added to the calculated loads. Also, due to growth expectations in future 25 % was also added to the loads. The dimensions for the wheel load used and the maximum and minimum static loads and dynamic braking loads are presented in tables 2 and 3 respectively.

Table 16 and 17 show the values for the wheel load geometry as well as the calculated loads for the main and nose wheel, respectively.

Table 16: Wheel Load Dimensions

Wheel Load Geometry Dimensions [ft]	
Ma	2.8
Mf	5.5
Na	28.3
Nf	25.6
B	31.1

Table 17: Wheel Loads

	Nose Wheel	Each Nose Wheel	Main Wheel	Each main wheel
Maximum Static Loads [lb]	5868.4	2934.2	40386	10097
Minimum Static Loads [lb]	2987.5	1493.8	3995.8	998.9577
Dynamic Loads [lb]	6093.9			

The landing gear also experiences a dynamic loading when the aircraft which is due to the acceleration and deceleration of the aircraft mainly during landing and take-off. The nose gear has to carry the dynamic braking during the landing operations when the aircraft is braking while the main gear carries the dynamic loading during takeoff. Hence the total main and nose gear load, which is the maximum static load plus the dynamic loading, is given by equation 9.13 from Mohammed Sadraey's book as:

$$(Max\ Loads)_{nose} = W\frac{M_f}{B} + \frac{10HW}{gB}$$

$$(Max\ Loads)_{main} = W\frac{N_a}{B} + \frac{10HW}{gB}$$

To also insure ground controllability it was important that the 'M_a', which is the distance from the main wheel to the aft Center of Gravity, of our tricycle landing gear was more than 5% of the wheel base, 'B', distance from the main wheel to the nose wheel. From the table 15,' M_a' was 2.8 which was more than 5% of the wheel base, 'B' which is 1.6 ft. The calculations are presented in table 18.

Table 18: Maximum Tire Loads

	Nose wheel Load(2)	Main wheel Load(4)
Maximum Load [lb]	6376.2	30862
Maximum Load per wheel [lb]	3188.1	7715.5

It is worth noting that the main wheel almost the total load of the aircraft of 33000lbs. during takeoff.

Next, the tire was chosen from the Goodyear tire data online[2].The tires were selected by choosing the smallest diameter rated tire that would carry the desired dynamic and static loads. The tires chosen to fit the loading of the main gear and the nose gear are shown in the table below.

Table 19: Final Wheel Dimensions

	Size [in]	Speed [kts]	Maximum Load [lb]	Rolling Radius [in]
Nose Tires	18X4.4	217kt	4350	7.9
Main Tires	28X7.7	174kt	11000	12.2

Therefore the wheel sizes for the nose and main wheel were 18 and 28 inches respectively. A tire supports a load almost entirely by its internal pressure. The important loads are the weight carried by the tire, W_w which was calculated by multiplying the pressure by the tire contact area with the pavement. They were calculated using the following Raymer's Equations:

$$W_w = PA_p \qquad Eq\ (11.5)$$

$$A_p = 2.3\sqrt{wd}\left(\frac{d}{2} - R_r\right) \qquad Eq\ (11.6)$$

The calculated pavement area for the main wheel was 58in^2 while the weight carried by the main wheel was found to be 4,057lbs, while the nose tire was found to have a pavement area of 9.4in^2 and to carry a weight of about 660 lbs. Since majority of regional airplanes operate in tarmac roads with good foundation, inflation pressure of 70 lb/in^2 was used.

The kinetic energy for braking was then calculated by using Raymer's equation 11.7.

$$KE_{braking} = \frac{1}{2}\frac{W_{landing}}{g}V_{stall}^2 \qquad Eq(11.7)$$

The landing weight is approximately 80-100% of the total take-off weight. Since sonata will be operating under FAR 25, the total takeoff weight was used instead. This is to allow for the aircraft to be able to land in the case of an aborted landing. The Kinetic energy for braking was found to be $24.8*10^6$ft-lb/s.

The shock absorber was used tin order for the tire to be able to absorb shock exerted on the structure during touchdown when landing. Tires help in shock absorption, but for medium and lighter planes, there has to be other structures to supplement the tires in shock absorption. The oleopneumatic shock absorber was used on sonata because it is the current mostly used shock absorber on planes today. This will also increase the chances of them performing on sonata. The oleo is simply a combination of a spring effect with mechanical coil spring and a hydraulic damper. For this plane a metered oleo was used, since it maximizes the efficiency by enabling the variation in the size of the orifice as the oleo is compresses. The oleo was also chosen because the landing gears used on the plane were retractable.

Stroke is the desired deflection of the shock absorbing system. It depends on the vertical velocity at touchdown, the shock-absorbing material and the amount of wing velocity at touchdown. The required stroke was calculated using:

$$S = \frac{V_{vertical}^2}{2g\,\eta N_{gear}} - \frac{\eta_T}{\eta} S_T \qquad Eq\ (11.12)$$

Where:
$V_{vertical}$ =10 ft. /s
η -Shock Absorber Efficiency, 0.75 for metered orifice
η_T-Tire Shock absorber efficiency
N_{gear}-3, Gear Load factor

The Stroke from the calculation was 5; therefore the stroke size given by Raymer of 12 inches was used for this aircraft.

After the stroke was determined, the oleo was sized. Oleo diameter is determined by the load carried by the oleo. The main oleo load in the main gear was determined by halving the value of the maximum static load, while the nosewheel oleo load was calculated by the addition of the static and dynamic loads which is given by the equation 4.

Table 20: Oleo Loads

Wheel	Oleo Load [lb]
Main wheel	20193
Nose wheel	6074

Finally the equation 11.13 in Raymer's text was used to calculate the oleo diameter.

$$D_{oleo} = 1.3\sqrt{\frac{4L_{oleo}}{p\pi}} \qquad Eq\ (11.13)$$

L_{oleo} was the load on the oleo that was calculated as has been explained above. The calculated oleo diameters for the main and nose wheels were found to be 4.9ft and 2.7ft, respectively, using internal pressure of 1800 lb/in^2.

Landing Gear

The design and placement of the landing gear is unique for each aircraft. The primary functions of the landing gear are as follows:

- They help in the aircraft stability during the ground and during loading, unloading and taxi.
- They help in the maneuverability of the aircraft especially during taxiing.
- They help to provide a safe distance from the ground, which is highly important for turboprop aircrafts such as sonata. This distance will prevent the damage of the propeller, wing etc.
- They help in the absorption of the shocks during aircraft landing
- They facilitate takeoff by allowing the aircraft to take off with the required acceleration as well as provide the rotation needed for takeoff with the lowest friction.

For the Sonata, the retractable landing gear was chosen mainly due to the fact that it reduces the drag during flight, which would translate to reduced fuel consumption and finally reduction of the flight for the passengers. The retracted gear should be able to retract to the aircraft without interference with other systems such the slipstream, fuel tanks and fuselage itself. Sonata will have a gear retractable to the nacelle of the engines. For this airplane, the main gears will be retracted into the engine nacelles while the nose gear will be retracted into the fuselage. This is acceptable since the aircraft being designed is a low wing.

For the landing gear, two tires were used in the nose wheel while four were used in the main wheel tires. The number of tires was used to ensure that there was still some control in the event of a flat tire and also for safety. The use of more tires also facilitates in the spread of the aircraft loads which would make it possible for smaller sized tires to be used. Use of two wheels on the nose also decreases the wheel frontal area which translates to better aircraft performance.

The preferred gear arrangement for the sonata is the tricycle gear. This was chosen because it is the most common used. In the tricycle gear arrangement, the wheels aft of the aircraft CG are very close compared to the forward gear. They also carry more weight. For this aircraft they carry 90% of the weight while the nose gear carried 10% of the weight. The main advantages of this landing gear system are:

- It allows the floor to be flat for passengers and cargo handling.
- It is directionally stable on the ground as well as during taxiing, which is because the aircraft tends to correct itself if, for example it is yawed from taxiing, it will go back on track due to the rolling and skidding resistances of the main gear that act behind the CG
- The pilot view is improved considerably, especially during takeoff and landing operations.

Propeller Sizing

In order to determine landing gear height and engine location, the propeller size must be determined. To determine the propeller diameter, equation 8.8 from Sadraey's book was used.

$$D_p = K_{np}{}^2 \sqrt{\frac{2P\eta_p AR_p}{\rho V_{av}^2 C_{L_p V_c}}}$$

Where:

K_{np}=0.72 for the six bladed propeller used

η_p-Propeller efficiency

AR_p-Propeller Aspect Ratio

ρ- Cruise density

V_{av}-Average airspeed for lift generation, typically $0.7V_{tipcruise}$

C_{LP}-Propeller Lift Coefficient

V_c-Cruise speed

The parameters were determined from the book as shown in table 21.

Table 21: Propeller Sizing

Propeller Sizing	
C_{LP}	0.4
K_{np}	0.72
η_p	0.8
AR_P	7
V_{av}	175
V_c	337.562
rho_{cruise}	0.001066
$V_{tipcruise}$	885.827

A six bladed propeller was used as opposed to a propeller with less number of blades because the more the blades the smaller the diameter. If a Propeller with a lower number of blades was used, then we would have had a propeller with very long blades which would necessitate more propeller clearance from the ground that would translate to a longer gear and hence a heavier plane.

From these parameters, the propeller diameter was found to be 13.4 ft. This was very close compared to our benchmarked plane, Dash 8, which has a propeller diameter of 13.5 ft.

After the calculation of the tip speed , the tip cruise speed was calculated by the equation given by Sadraey as:

$$V_{tip_{Cruise}} = \sqrt{V_{tip_{static}}^2 + V_C^2}$$

Where the static prop tip speed was calculated by the equation:

$$V_{tip_{Cruise}} = \frac{D_p}{2}\omega$$

Where ω the propeller rotation is speed in rad. /sec. and is given by the equation:

$$\omega = \frac{2\pi.n}{60}$$

The results from these equations are given below:

Table 22: Prop Parameters

Prop parameters	
D_p [in]	13.4
$V_{tip_{Stat}}$ [ft/sec]	222.9639
ω [rpm]	1041.2
n_p [rpm]	1200
GR	0.8677

The Pratt and Whitney engine used in this aircraft has an angular velocity of 1200 revolution per second. It was used to determine if the power supplied to the propellers will exceed the required power. This is important to ensure that the tip speed does not exceed the speed of sound as it would create shocks on the propeller tip which would lead to a considerable increase in drag especially during high speeds. Since the engine shaft speed exceeds the prop rotational speed, a gear box was used to reduce the speed to the required speed. The Gear Box Ratio is given by:

$$GR = \frac{\eta_p}{\eta_s}$$

The calculated value of the gear box ratio was 0.8677. The propeller used was a metal regular propeller with a tip speed of 222.9639 ft/s.

Performance Analysis

The performance of sonata was calculated using the averaged cruise weight, power and aircraft geometry. A program was written to help in the determination of the important performance parameters. The main parameters were: the cruise coefficient of lift, velocities for maximum

cruise, range and loiter, minimum sink rate and its velocity, maximum glide range and its velocity and finally the service ceiling. In order to do these we needed two important parameters: the zero lift drag coefficient (C_{D0}) and the coefficient of drag due to lift (K). These two parameters were based on the benchmarked planes, and a value of 0.0376 and 0.0255 were used for the K and C_{D0} respectively. The performance parameters were then calculated using the equations below.

$$\left(\frac{L}{D}\right)_{max} = \left(\frac{C_L}{C_D}\right)_{max} = \sqrt{\frac{1}{4C_{D,0}}}$$

$$V_{\left(C_L^{3/2}/C_D\right)_{max}} = \left(\frac{2}{\rho_0}\sqrt{\frac{K}{3C_{D,0}}}\frac{W}{S}\right)^{1/2}$$

$$\frac{P_A}{(P_A)_0} = \left(\frac{\rho}{\rho_0}\right)^n \qquad Where\ n = 0.7\ for\ the\ turboprop$$

$$\left(\frac{C_L^{3/2}}{C_D}\right)_{max} = \frac{1}{4}\left(\frac{3}{KC_{D,0}^{1/3}}\right)^{3/4}$$

$$(R/C)_{max} = \frac{\eta_{pr}P}{W} - \left[\frac{2}{\rho_\infty}\sqrt{\frac{K}{3C_{D,0}}}\left(\frac{W}{S}\right)\right]^{1/2}\frac{1.155}{(L/D)_{max}}$$

$$V_{(R/C)_{max}} = V_{\left(C_L^{3/2}/C_D\right)_{max}} = \left(\frac{2}{\rho_\infty}\sqrt{\frac{K}{3C_{D,0}}}\frac{W}{S}\right)^{1/2}$$

$$\theta_{min} = \tan^{-1}\frac{1}{(L/D)_{max}} * \left(\frac{2\pi}{360}\right) \qquad in\ degrees$$

$$V_{(V)_{min}} = \sqrt{\frac{2}{\rho_\infty\left(C_L^{3/2}/C_D\right)_{max}}\frac{W}{S}} \qquad minimum\ sink\ rate$$

$$(V_\infty)_{minsinkrate} = V_{\left(C_L^{3/2}/C_D\right)_{max}} = \left(\frac{2}{\rho_0}\sqrt{\frac{K}{3C_{D,0}}}\,\frac{W}{S}\right)^{1/2}$$

$$R_{maxglide} = \frac{h}{\tan\theta_{min}}$$

$$V_{(glide)_{max}} = V_{\left(C_L^{3/2}/C_D\right)_{max}} = \left(\frac{2}{\rho_0}\sqrt{\frac{K}{3C_{D,0}}}\,\frac{W}{S}\right)^{1/2}$$

$$R_{max} = \frac{\eta_{pr}}{c}\left(\frac{L}{D}\right)_{max}\ln\frac{W_0}{W_1}$$

$$E_{max} = \frac{\eta_{pr}}{c}\left(\frac{C_L^{3/2}}{C_D}\right)_{max}\sqrt{2\rho_\infty S}\left(W_1^{-1/2} - W_0^{-1/2}\right)$$

Table 23: Performance Results

Performance parameters	
Cruise CL	0.43
$(L/D)_{max}$	16.1475
$(CL^{(3/2)}/CD)_{max}$	16.7015
$V_{(L/D(max}$ -(ft. /sec)	267.3175
$V_{(CL^{(3/2)}/CD)max}$ – (ft./sec)	203.1174
Range Specific fuel consumption (1/ft.)	$2.53*10^{-7}$
Loiter Specific fuel consumption (1/ft.)	$3.03*10^{-7}$
Maximum Range (nm)	773.2
Maximum endurance (hrs.)	3.2
Minimum Glide angle (deg.)	3.5
Max. glide range (ft.)	1548
Vel. $(R/C)_{max}$- (ft./sec)	203
Maximum (R/C)- ft. /sec	63.4

The Service ceiling was calculated by solving for the density that will result in a maximum rate of climb of 1.67 ft. /sec. From there the altitude for the required density was checked from density-altitude charts. The equation used is given below.

$$\rho_\infty = \frac{2}{\left[\frac{3C_{D,0}}{K}\left\{\frac{S}{W}\left|\frac{(L/D)_{max}}{1.155}\left(\frac{\eta_{pr}P}{W}-(R/C)_{max}\right)\right|^2\right\}^2\right]^{1/2}}$$

After solving a density of 0.00097654 slug/ft.^{3} was found. From the density-altitude charts, this is given by an altitude of approximately 28,000 ft.. The absolute ceiling is so important because it determines the flight envelope of the aircraft. It is the maximum altitude which the aircraft will be able to maintain level flight. It was calculated from the above equation, with the maximum rate of climb having 0 ft. /sec. The absolute ceiling density was 6.4*10^4 slug /ft.^{3}, which translates to an altitude of 38,000 ft.

The specific fuel consumptions for the range and loiter calculations were calculated using the equations from Raymer's text. First, the equations were converted into consistent units and then plugged into the performance equations which were given before.

$$C_{range} = \frac{0.5\frac{lb}{h.bhp}}{\left(550\frac{lb.ft}{sec.} * 3600s.\right)}$$

$$C_{endurance} = \frac{0.6\frac{lb}{h.bhp}}{\left(550\frac{lb.ft}{sec.} * 3600s.\right)}$$

The values 0.5 and 0.6 for the specific fuel consumption were chosen from Raymer's book in table 3.4. The conversions were done to convert the units to ft^{-1} which were then used in the range equations. The units were analyzed to ensure that they give the answers in the correct units.

In order to get the maximum velocity, a graph was used to calculate the maximum cruise velocity, which was the point where the Power Available and the Power Required curves intersected.

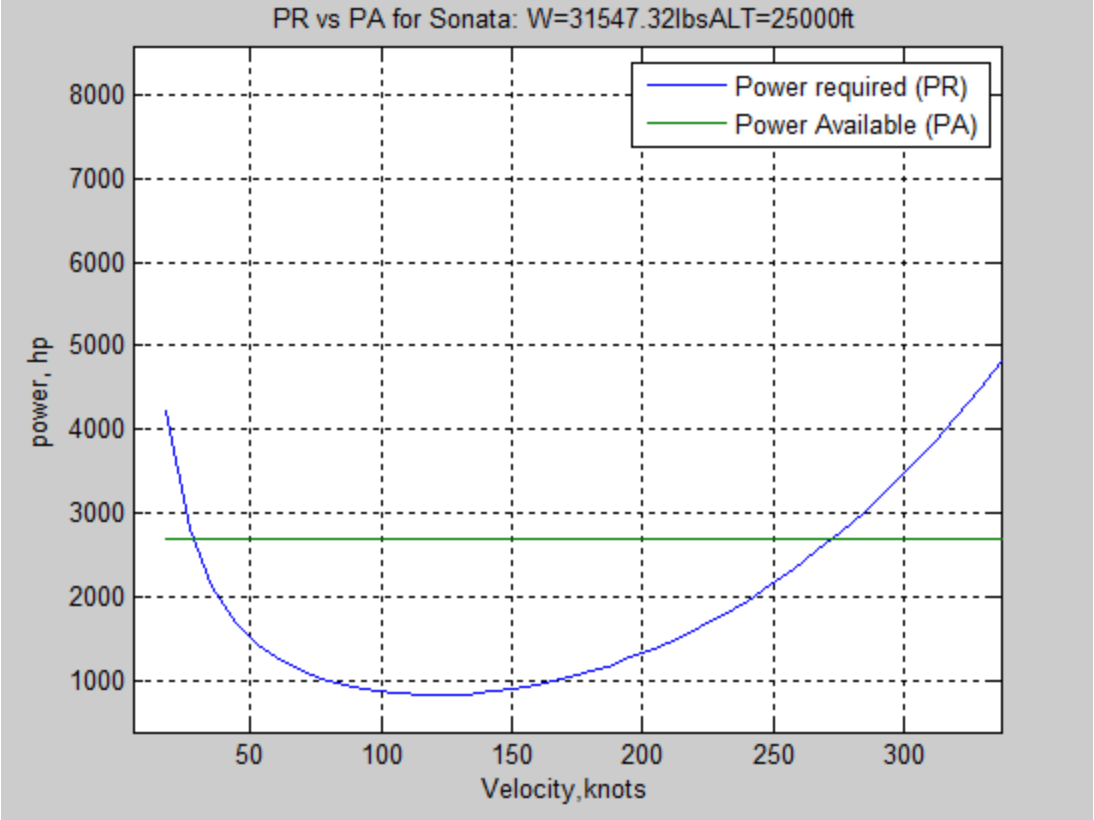

Figure 2: Power Curves at Cruising Altitude

From here the cruise speed was found to be approximately 270 knots which is very close to the Dash 8 which has a cruise velocity of 265 knots. This cruise speed is at maximum $\frac{L}{D}$ which gives the maximum range and the most efficient flight.

Final Design: Sonata

With the overall configuration and features decided on after the conceptual design phase, work shifted to refining the aircraft for stability, CG, weight, performance, and sub-system integration. This process necessitated various changes which can be seen in the drawings. These changes include adjustment of the engines for stability and CG, moving the wing for balance and adjusting of the static margin, and finally adding detail features.

The overall configuration of the fuselage remained largely unchanged from conceptual to preliminary design stages. However, the galley, attendant seats, lavatory, and closet were moved about for stability as needed to ensure the main entrances are clear of the propellers. Note though that in the process of stabilizing the aircraft, the wing moved forward enough that there could be a tail-tipping problem when loading cargo into the rear cargo door. Therefore a

useful subsystem that should be added during structural design is a stowable stand to support the tail during cargo loading.

Aft fuselage up-sweep during conceptual design was estimated at 20 degrees. During the process of preliminary design, this reduced to 16 degrees. This is still adequate for allowing the pilot to pitch as much as he may need while limiting the possibility of a tail-strike. The pilot visibility would be slightly improved over the conceptual design as the nose length forward of the cockpit was slightly reduced and the floor of the cockpit was raised above the level of the cabin floor. While there was a specific distance it was raised, the actual and final value will be left until it is clear how much over-head space is required in the cockpit for controls.

The final external dimensions of the aircraft can be seen in the following table.

Table 25: Final Dimension Summary

Wing Area [ft^2]	Span [ft]	Length [ft]	Height [ft]	AR	C_bar [ft]
1005.5	100.3	88	34	10	10.2
Root Chord [ft]	**Tip Chord [ft]**		**Fuse Diam [ft]**	**VT [ft^2]**	**HT [ft^2]**
12.4	7.6		9.25	150	171
Empty Weight [lb]	**MTOW [lb]**		**Fuel Weight [lb]**	**C_D0**	**C_Lmax**
21749	34202		5063	0.023	2.14

Fuselage

The fuselage length is derived from the internal volume requirement imposed by the passengers and baggage. The internal layout was optimized to maintain the preferred fineness ratio of about eight. This meant creating an asymmetric seating arrangement, with two seats on one side of the aisle and one seat on the other. Each row is 21.8in apart, five additional feet are added aft of the last seat for one of the attendant seats and for an emergency door on both sides of the fuselage. Seven feet are added forward of the first seat for the other attendant seat, the lavatory and galley, and a door on both sides of the fuselage. This creates a 44ft cabin length.

The diameter of the aircraft was next determined. Each seat is 1.5ft wide, totaling 4.5ft across for all seats. The aisle is mandated by the FAA as at least 20in wide, or 1.67ft. Adding an additional 6in to each side to provide head clearance for a rounded fuselage, adds another foot. The wall thickness of the fuselage will be at least 6in for adequate structure and room for

wiring or other cables. Lastly, there will be a little more than a foot added for arm rests and slight seat separation for added comfort. This provides a total fuselage diameter of 9.25ft.

There is added thickness below the fuselage for wing and systems placement. By placing the wing below the fuselage, the internal cabin can go uninterrupted by spars and other structural members. This added thickness provides a fuselage depth of 10.9ft.

The desired fineness ratio of eight pushes the total length of the aircraft to 76ft. This is increased to ensure that there is enough room for adequate baggage room, totaling 88ft. The remaining length of the fuselage outside of the cabin area constitutes the additional 44ft. The baggage compartment must be able to hold $121ft^3$ of volume. This is determined from what modern airliners consider to be a normal sized bag, with a volume of $2.78ft^3$. Assuming every passenger has at least one bag, and then adding an additional 25% to account for multiple bags, oversized bags, or oddly shaped cargo, sums to the provided $121ft^3$. The baggage compartment is located aft of the main cabin area, below the leading edge root of the tail. This limits the height of the compartment, causing it to be longer in the x-direction. Assuming only 30% of the diameter is usable in this location, due to a desired flat bottom surface and the tail structure; the baggage compartment will be about 6ft long. This provides $150ft^3$of volume, meeting the requirement.

This leaves about 17ft forward of the cabin area for cockpit and other components that are typically fitted in the nose, such as avionics and weather radar.

Tail Sizing

Using the equations explained above, the tail area is found. The moment arm used is now fixed per the stability analysis. Original estimates provided a desired vertical tail area of somewhere between $126.9ft^2$ and $139ft^2$. The horizontal tail area is between $132.2.ft^2$ and $145.5ft^2$. The design horizontal area is $171ft^2$, about 90% of what was calculated earlier in the analysis section. The vertical tail area is $150ft^2$, again 90% of what was calculated. Both of these values are a result of tens of iterations of stability analysis ensuring that the aircraft was stable in all flight regimes. The distance between the wing MAC and the horizontal tail MAC is 47.5ft and the vertical tail MAC is 49.7ft aft.

Propeller

Fully Feathering- helps to stop the rotation of a non-operational engine. This will help to reduce the drag and vibration of the engine. It also prevents the inoperative engine from wind milling. This is achieved by turning the propeller to a high pitch which enables the blades to be parallel to the airstream.

Reverse-pitch- help in the reduction of landing distance, that is the landing roll. It does this by reversing the thrust during landing which when used with the landing gear reduces the overall landing distance.

The diameter of this propeller is 13.5ft.

Airfoils

The same airfoil described in the conceptual report, the NACA 4415, is used for the main wing. It was found that this airfoil had the needed performance characteristics, as well as internal volume for fuel capacity. Xfoil was used to analyze the airfoil at various Reynold's numbers and angles of attack. Different flap angles were also examined in order to accurately represent the airfoil in the code. The maximum lift coefficient is about 1.9 and occurs at an angle of attack of 18 degrees. The increase in lift with angle of attack is about -6.36 per radian. The effect of flaps on the lift is an increase of 2.14 per radian of flap deflection, or .037 per dgree. This provides sufficient lift and is slightly higher than what was initially used in the conceptual design.

The tail surfaces feature a NACA 0010 airfoil. Symmetry is desired so little lift is produced when in level flight. A large thickness similar to the main wing is not needed since nothing is to be placed inside of the tail surfaces, with the exception of structural elements and small actuators for the controls.

The bulk of the Xfoil analysis of the airfoil was conducted in the conceptual design phase and therefore will not be included in this report.

Control Surfaces

The control surfaces are sized here according to historical values. The aileron span to wing span is ratio is designed at .3, resulting in an aileron chord of about .35. The small ailerons are aided in roll control from the addition of spoilers. While the rudder and elevator chord ratios were originally sized to that of a historical jet transport, stability analysis eventually was what drove the final sizing. This resulted in an elevator chord ratio of .4 and a rudder area ratio of .3. Both are slightly overhung for lighter pilot controls.

The influence of elevator deflection on lift produced was found using Xfoil as well. It resulted in an increase in lift of 3.89 per radian deflected, .068 per degree.

All above dimensions and design calculations were then handed off to the draftsman for scaled drawings and models to be created.

Internal Arrangement

Key component locations are explained here as located by the stability calculations. Each location given in the CG table showed earlier represents where the CG of that respective component was expected to be, measured aft from the nose. The fuselage weight was located slightly forward of the midpoint of the body since the bulk of the structure will be located at the wing junction. The wing weight is located at about the 30% chord line due to most of the weight being centered on the main spar at the quarter-chord. Components including flight controls, hydraulics, electrical components, and air conditioning are spread out amongst the entire aircraft and have representative placements based on the stability analysis. The detailed design will ensure that these components are spread out properly. The main components, such as hydraulic fluid storage, or pneumatic cylinders, are stored in the belly bulge under the fuselage. Refer to the modeling section to visualize the large open space there for this purpose.

The engines, starter, fuel systems, fuel, nacelles, and engine controls are located on or in the wing. The fuel tanks are placed here to reduce the amount of fuel piping needed, thus reducing overall weight. The engines and starters are located in the forward half of the nacelles, with the engine controls and all other connections located in the upper aft section, above the main gear. The main landing gear retracts forward into the nacelle, reducing weight by placing two structural hard-points at one location. The fuel tanks have a cumulative volume of 809 gallons, greater than the 750 required to allow for adjustment of aircraft performance/requirements later.

Instrumentation, avionics, lavatory, galley (furnishings), and pilot seats are all located in the forward section of the aircraft. The galley and lavatory were originally to be placed one in front and one in back, but stability required they both be placed forward of the wing, in order to open up space behind the cabin for the heavier baggage compartment. The APU is also located in the tail section of the plane for stability. Its large weight allows for the designer to move it wherever possible to shift the CG.

Anti-icing equipment is located on the wing and both tail surface leading edges, as well as the propeller blades. The weight location is an average of the four.

Structures

At this stage of the design process structural design was limited to conceptual. Therefore only brief descriptions of fuselage structural members and a general conceptual model of the spars is shown in the modeling section.

Structural design would be the next step in the design process after yaw stability analysis is complete.

Design Modeling

Ultimately what is built is what is drawn. Therefore care should be taken to develop proper models both on paper and scale in order to clearly communicate the overall shaping of the aircraft to be built. In the case of this project, at the start a scale model was constructed of the conceptual design or so called 'dash one' configuration. After extensive stability and CG analysis as well as refined weight and cost analysis, the design is adjusted. This evolution can be clearly seen with the change from the scale model to the final design SolidWorks virtual models in particular with wing location and nacelle locations.

A key part of the aircraft design phase is to ensure there is enough volume inside the airframe to house all that must be housed. This includes people, avionics, fuel, engines, landing gear, and many other components. Thus in the virtual model, rough approximations of some of these were created to further guide the adjustment of the design to something more realistic. As this is occurring, virtual modeling allows for accurate tailoring of the CG by way of moving components and checking for interferences. Considering safety, the door location became an issue. The main passenger entrance should be located fore of the prop arc yet moving it too far forward can interfere with the cockpit arrangement. In particular the adjustment of doors and seats benefited greatly from the use of a 3D model.

After the stability analysis the design was frozen. Access panels and control surfaces were then added to the model. The access panel arrangement could change with further development however for now the currently represented panels cover some key areas.

The virtual model also allows for quick determination of the maximum rotation angle on the ground. The goal in conceptual design was twenty degrees however with this configuration sixteen degrees is the maximum rotation angle.

Note that the spars pass completely underneath the cabin minimizing discontinuities in both the wing structure and main fuselage structure.

Also note the ventral strakes added to the aft fuselage as was defined in the conceptual design phase.

A potential addition for future development is a stowable stand to be positioned in the extended position below the aft fuselage. This should be done to ensure the aircraft does not tip on to its tail during cargo loading through the rear hatch as the main landing gear far ahead of the cargo door.

Figure 3: Conceptual design scale model built of balsa wood

Figure 4: Iso view of preliminary design

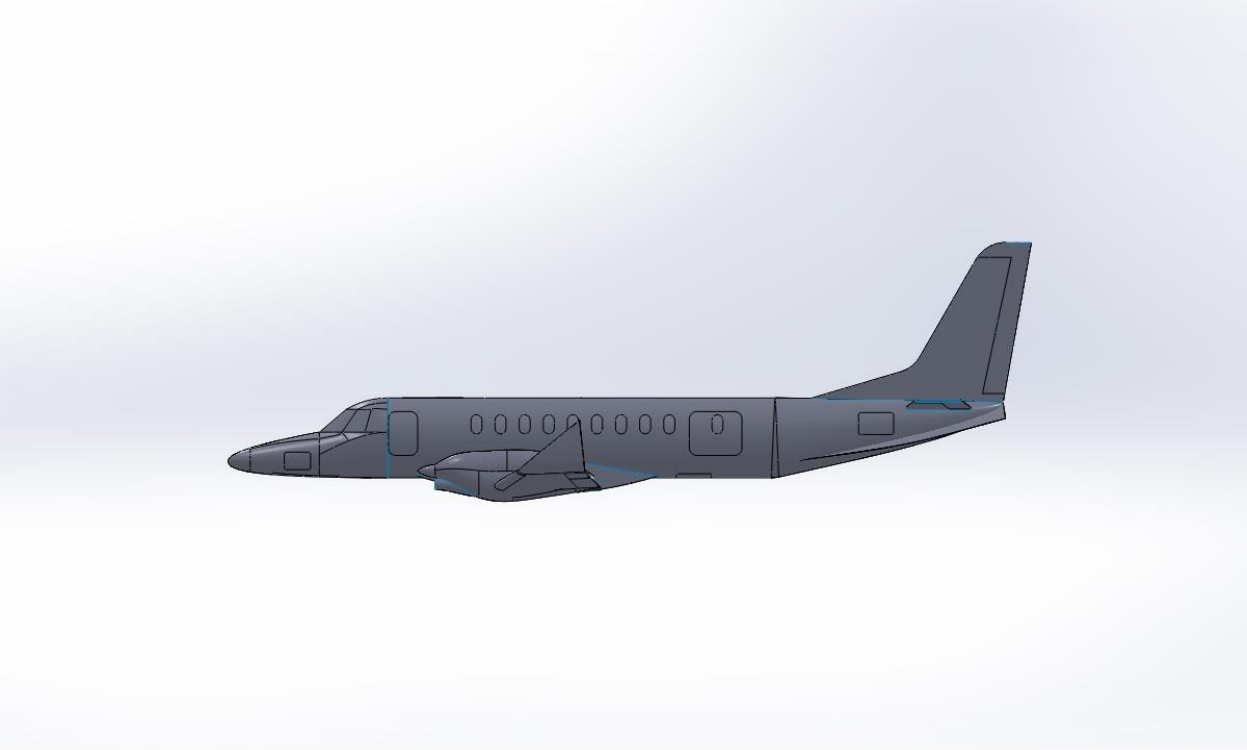

Figure 5: Side view

Figure 6: Opposite side view

Figure 7: Front view

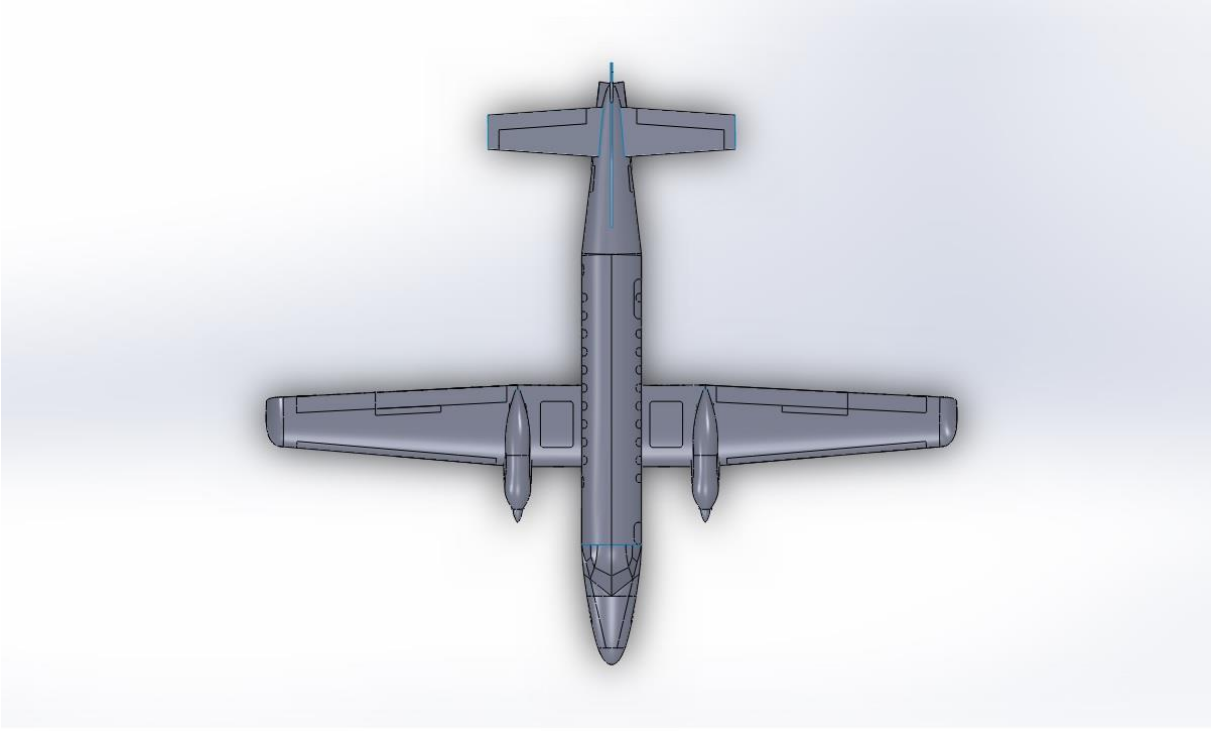

Figure 8: Top view

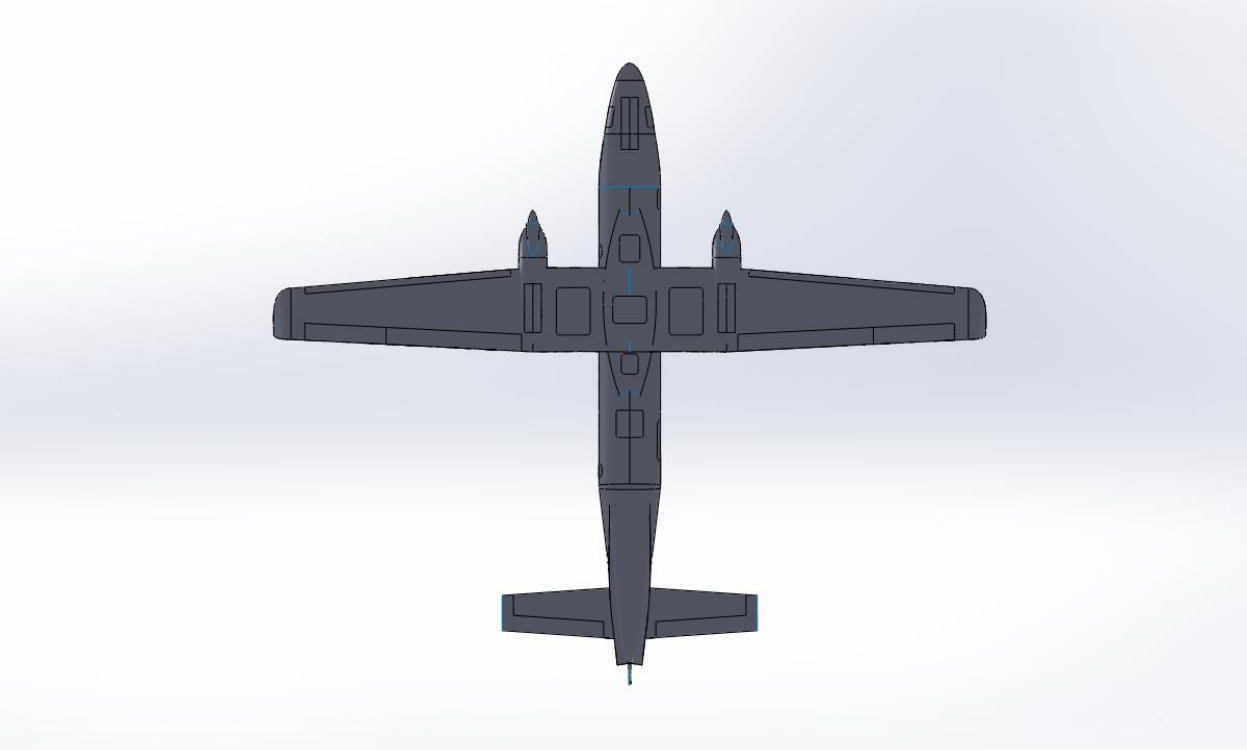

Figure 9: Bottom view

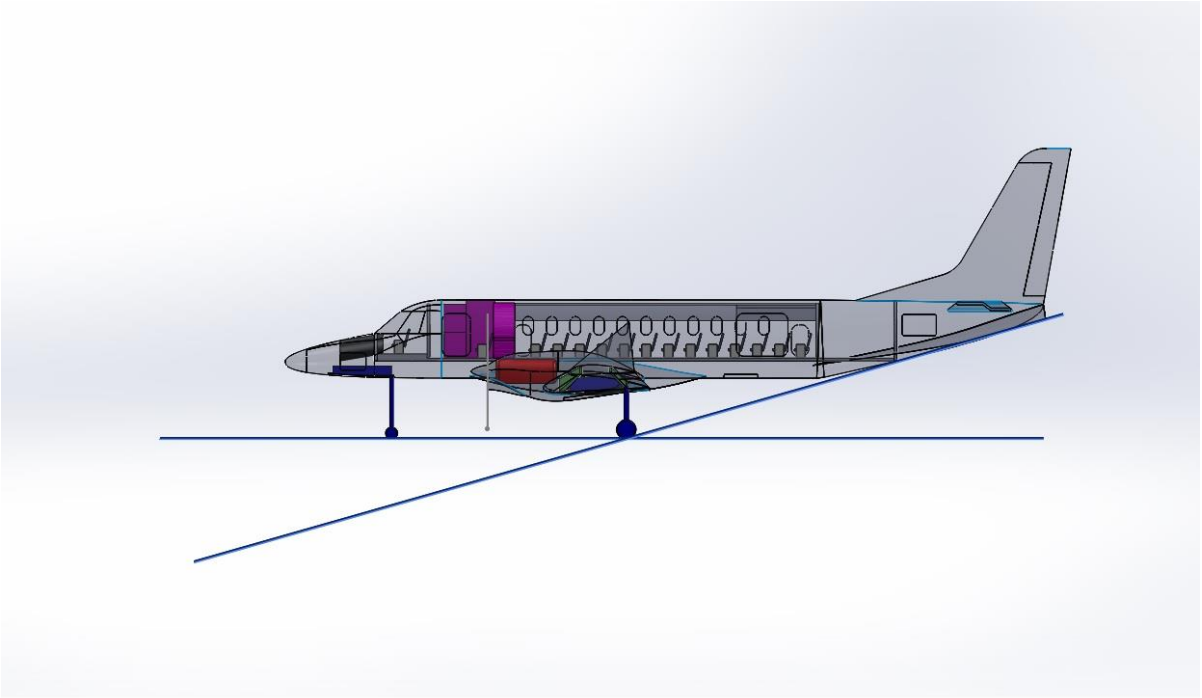

Figure 10: Side view depicting gear, engines, seats, lavatory, galley, closet, avionics, spars, wing tanks, and landing gear bays

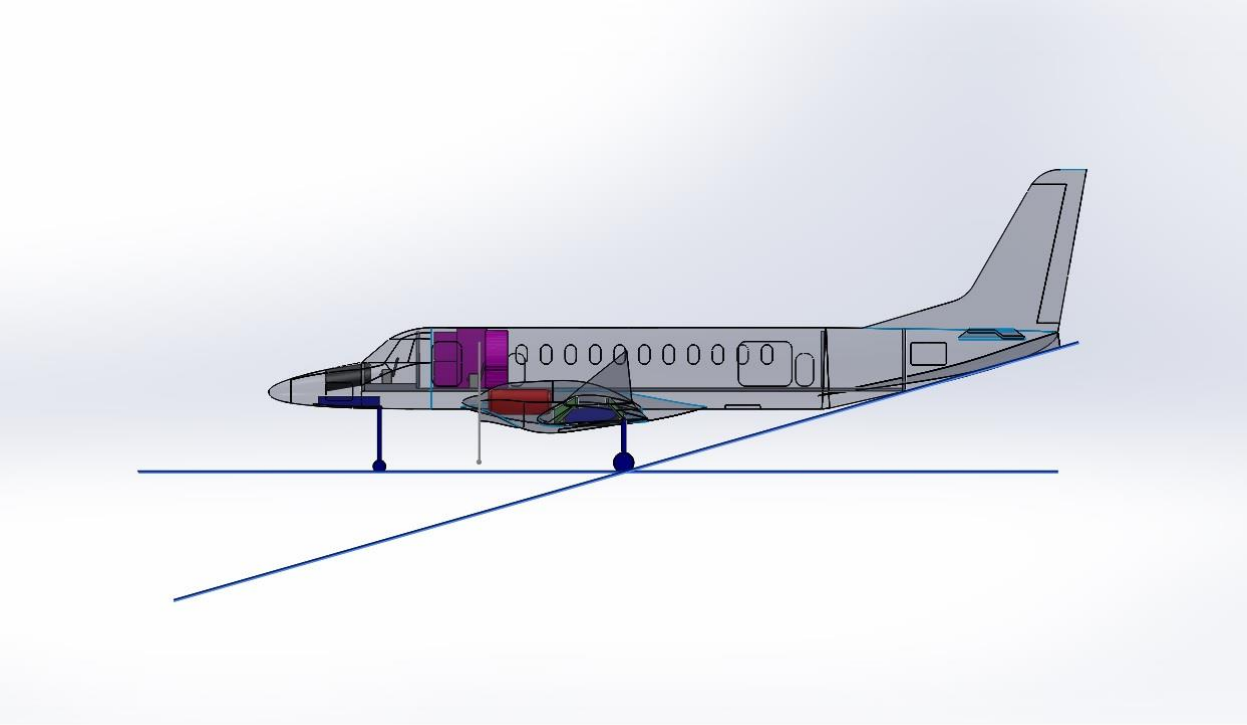

Figure 11: In cargo configuration maintaining galley, lav, closet, and fore attendant seat

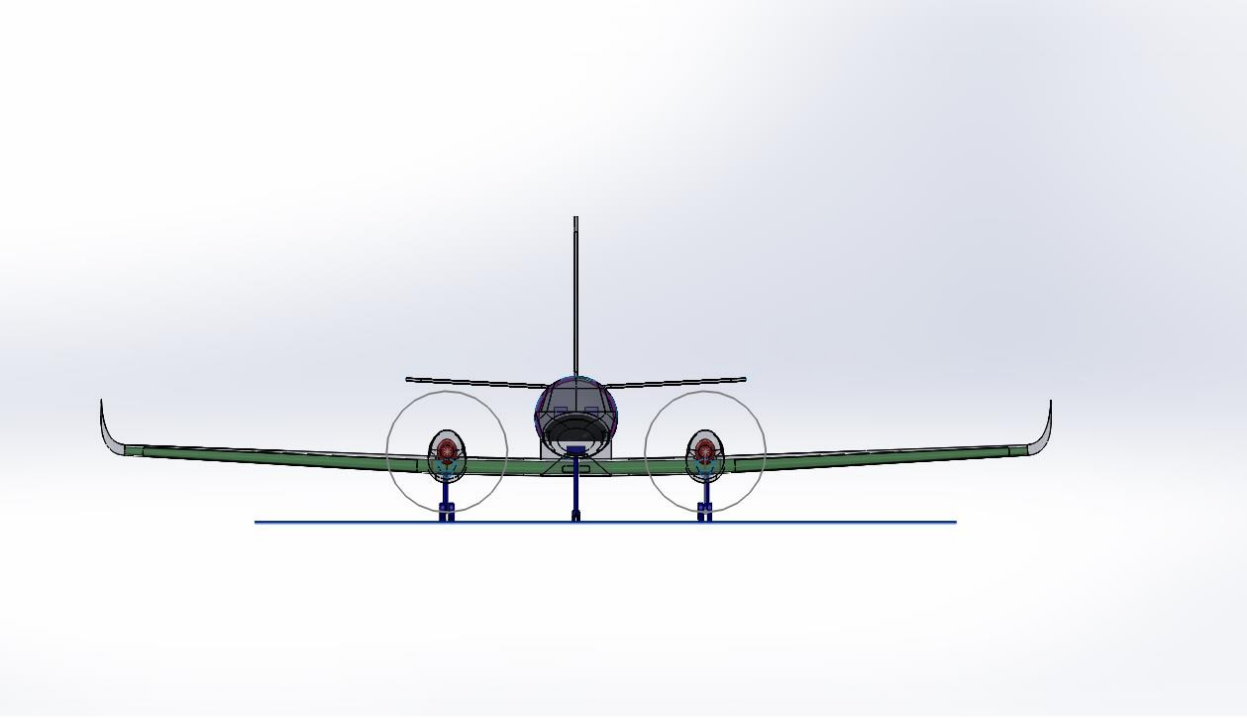

Figure 12: Front cutaway view

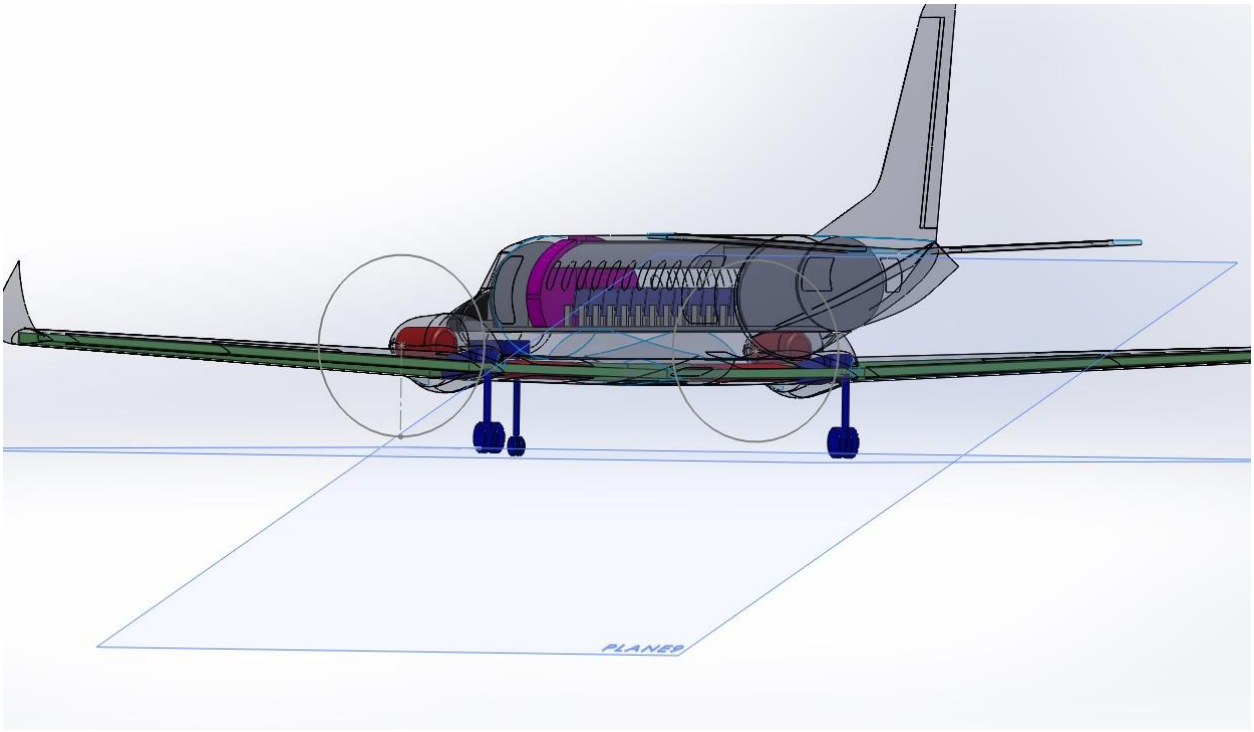

Figure 13: Note the genorous amount of open volume below the cabin floor and above the wing. This provides ample room for various components and growth room.

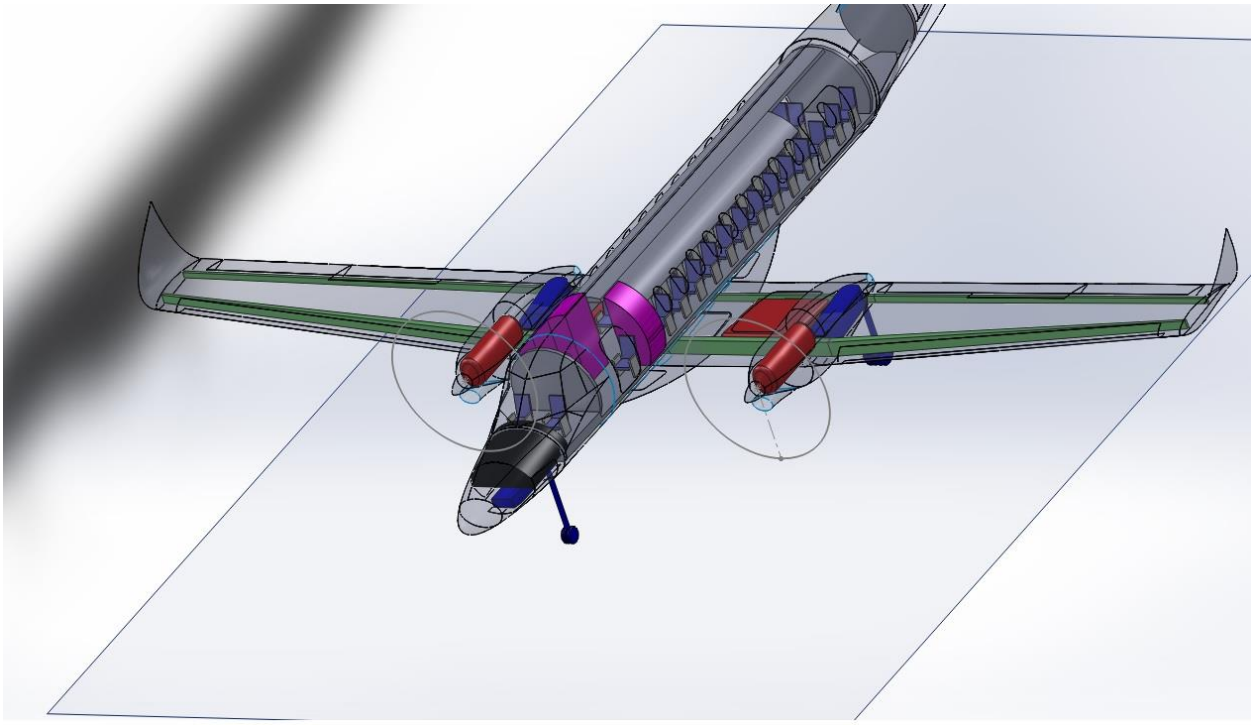

Figure 14: Closer Iso view near cabin entrance.

Cost Analysis

Using methods described in chapter 18 of Raymer's text, the RDT&E were estimated; RDT&E being Research, Development, Testing, and Evaluation. The equations used to estimate the costs will not be covered in detail in this report. The reader is directed to Raymer's text, chapter 18 for details. These equations are statistically based however and may not necessarily be correct.

The cost analysis methods for RDT&E use the DAPCA IV method (Development and Procurement Costs of Aircraft). The general procedure used in the DAPCA method is to estimate the hours for manufacturing, maintenance, flight hours, and block hours. These hours are then multiplied by a rate for each category then added together. Key aircraft parameters that affect the cost in the DAPCA method are as follows:

- Empty Weight
- Maximum Velocity
- Expected production quantity
- Number of flight test aircraft
- Total number of engines required for production
- Avionics cost per-pound
- Cruise velocity
- Takeoff gross weight

For maintenance, the key variables are as follows:

- Number of engines per plane
- Cost per engine
- Aircraft cost less engine costs

The cost of Sonata is also affected by other cost additions such as a 'fudge factor' of 1.1 as provided by Raymer's text to account for an increase in the manufacturing time required for composites. Although Sonata is not an all-composite or even major-composite aircraft, composites are still used in places such as the winglets, access panels, doors, and other miscellaneous components. The bulk of the structure is still the standard aluminum build-up comprised of bulkheads, formers, and stringers. A brief side note on materials, a potential aluminum alloy of interest in the future is aluminum-lithium as it uses the same manufacturing processes as aluminum yet is still lighter and stronger. At the time of this writing, it appears to

only be used in fighter aircraft according to Raymer's text. Thus this exotic alloy might raise the cost above acceptable levels but could potentially be used in future production runs.

The wing is divided into three sections with the middle section lying between the engine nacelles and main landing gear. The outer wing sections will be attached at the built-up junction of the nacelle and main gear. As the center wing section lies entirely below the bottom of the fuselage, these components can be built separately during the bulk of construction. This can potentially decrease factory floor space, personnel, and equipment needed to move a partially constructed aircraft around the factory. Along this line, Sonata could be built in entirely separate smaller sub components coming together for final assembly at the last moment. This could also allow for extensive sub-contracting to reduce needed in-house infrastructure. Tail surfaces are attached in the traditional fashion to the rear fuselage. Due to this compartmentalization of construction, it is also possible to stretch Sonata to seat more as it is also possible to increase the wing span by attaching longer outer wing sections. This allows for growth opportunities in the design.

Note that the max velocity had a pronounced effect on cost per aircraft as did the total production run. As the production run is an expected market share, the maximum velocity will be the parameter adjusted to change price per airframe. Given that the cruise is 210kts, it is feasible to restrain the max speed to something as low as 220kts to reduce cost. Given the amount of power Sonata has available, the max theoretical speed is 325kts but building for 325kts adds approximately $3million to the price per aircraft. A plot is shown below depicting this relationship and the second figure depicts the rising costs for maintenance:

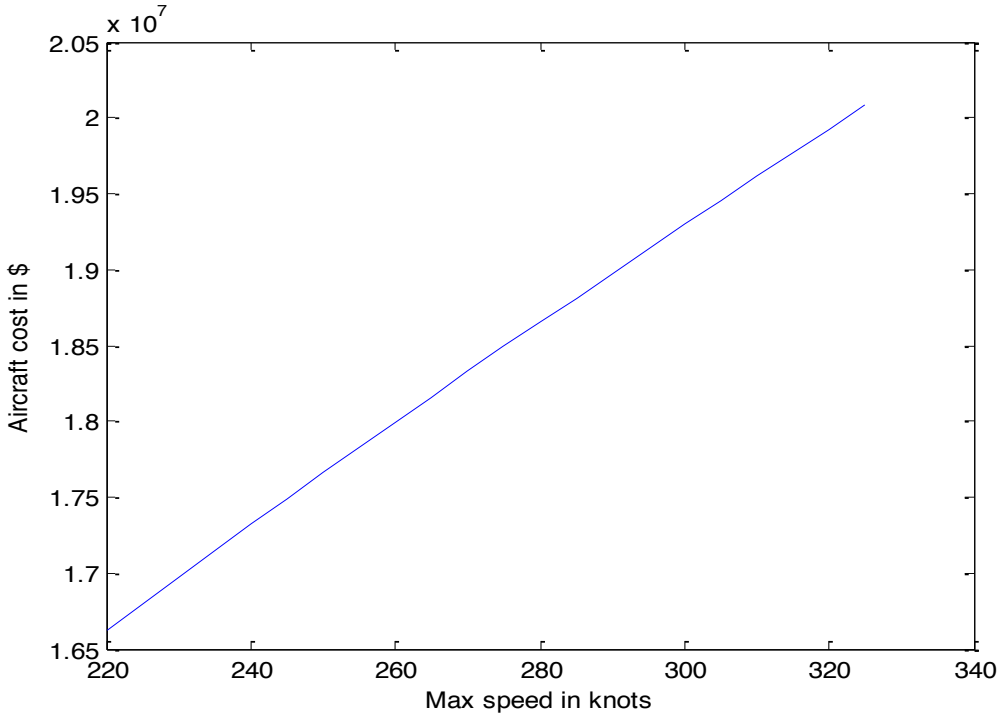

Figure 15: Aircraft Unit Cost

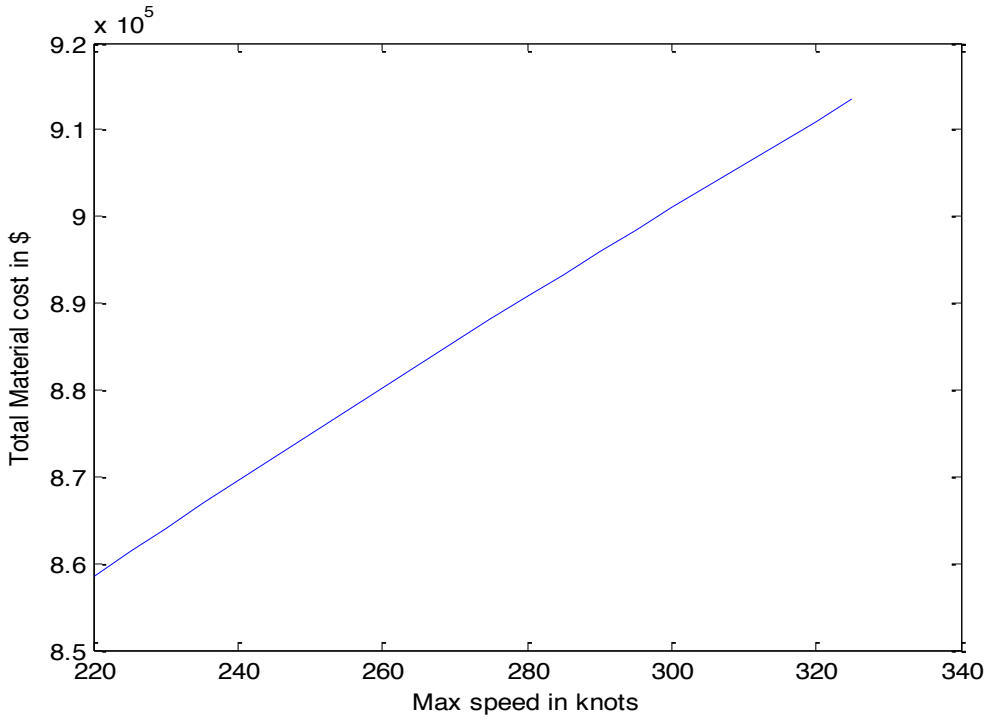

Figure 16: Total Material cost variation with max speed

The reader is asked to refer to the MATLAB code appendix for more detail on the procedure and input parameters however a table or some important inputs and preliminary calculations is presented below:

Table 26: Cost Parameters

Empty Weight (We in lbs)	21552
Avionics Weight (Wavionics in lbs)	1235
Production Quantity	200
# of Flight Test Airframes	2
Cruise Velocity (Vc in knts)	210
Takeoff Gross Weight (Wo in lbs)	34202
Number of Passengers	35
Number of Engines per plane	2
Number of Engines for production	400
Cost of Avionics (in $ per lb)	6000
Total Cost of Avionics	7,410,000
Cost of Engine (PW127G est)	2,000,000
Total Cost of Engines	800,000,000
Jet A prices per gal (at KBTL)	6.39
	Rates ($/hr)
Engineering	115
Tooling	118
Quality Control	108
Manufacturing	98
Two-Crew yearly salary	1,489,600
Three-Crew yearly salary	2,036,900

NOTE: All dollars are in 2012 dollars

Design Potential

'Sonata' is the product of a focus on low development cost, risk and ease of maintenance. However, it is also designed with potential modifications in mind. These modifications can include increasing the fuselage and cabin lengths by adding a 'plug' fore and aft of the wing which can increase the passenger capacity while maintaining the same wing, tail surfaces and by adding fore and aft, CG is maintained. A belly pack can also be added for additional fuel tanks or additional baggage space much like on the Cessna 208B, some Jetstreams, as well as some Beech 1900s. Also, the wing is in three sections with the center section running between the engines and mounts to the fuselage with each wing section outboard of the engine being another section. Thus the span can be increased or decreased easily without changes to the rest of the design.

'Sonata' also features a cargo door on the aft port side and would have removable seats allowing for the aircraft to be easily re-configured for different passenger configurations, seats can be removed for cargo operations, or a combination of payload layouts. The cargo door is also easy to access for loading operations. Given that reducing payload can increase range, if the customer decides to reduce the number of passengers this is possible. Given the way engines are mounted on the wings, engines can be changed as well to accommodate a weight growth via larger engines.

Design Recommendation

Design risk is an important part of the design process. Given that all aspects of a production aircraft must be validated before it can enter service, the more new technologies present the greater the development period and cost. This can directly affect profitability of the aircraft. Thus the simple and traditional design layout of the 'Sonata' would carry the least risk and be much cheaper to develop and certify for transport operations.

Individual Responsibilities

Brian Omondi Asimba

Responsibilities included engine selection, propeller selection, benchmarking research, and all associated FAR regulations, gear sizing, and performance. Provided these choices to Jacob for modification to the analysis and to Adam for updated sketching and implementation into the design, checking for feasibility.

Adam Houtman

Responsibilities included conceptual sketching, final drawings, 3D solid modeling, actual solid model, design choices, FAR requirements, and overall knowledge of aircraft marketing. Designed the internal layout, made most final decisions regarding key component locations, while taking feedback from other members. Adjusting drawings to meet analysis driven requirements.

Jacob Maynard

Responsibilities included analysis procedure, computer code writing, airfoil selection, FAR requirements, actual solid model, and report formatting. Majority of the math and aerodynamic analysis was completed here. Relayed equation driven design restraints to Adam, then adjusted and reran analysis based on feedback. Initial design variables based on benchmarking done by Brian.

ABET Outcomes

6) An ability to function on multi-disciplinary teams

This outcome is met by the division of labor amongst the group members. The total scope of the project was analyzed by the group as a whole in order to break it down and disperse responsibilities evenly, while considering individual strengths for project efficiency. After dividing the workload, meetings were scheduled multiple times a week in order to evaluate each other's progress, providing a check on the work being done. Consistent communication was maintained throughout the project.

7) An ability to identify, formulate, and solve engineering problems

Throughout the design process, downwind effects of each decision had to be considered. For example; if the engine is moved forward to shift the CG, how does the new prop location affect the door location as well as how moving the door affect the seating arrangement and so on. It was imperative that the group recognize these problems and solve them as they are introduced as well as mitigate the creation of downwind effects.

9) Knowledge of contemporary issues

All throughout the design process the team had to consider problems facing the airline industry today, as well as ergonomics. Passenger aircraft must be economical yet safe and comfortable for the passengers, comfortable for crew (to lower fatigue), and emergency situation safety must be considered with aisle size and exit locations. Current prices of this aircraft class were also examined for comparison.

APPENDIX A) Benchmarked Aircraft

Embraer Emb120

		Embraer Emb 120
Purpose of Aircraft		Transport
W-0(Max Takeoff weight)		25,353 lbs(11,500 kg)
W-e (Empty weight)		15,587 lbs(7,070 kg)
We/W0		0.62
Payload		Max=7319 lbs(3320 kg)
Passengers(Total Weight of Passengers)		30+2 crew
General dimensions	Length of aircraft	65.5ft (20.00m)
	Height of aircraft	20.8 ft (6.35 m)
Engine(s)	Number	2
	Type(Turboprop)	Pratt & Whitney Canada PW 118
	power	1800 shp(1324 kwt)
	Location(eg. Wing mounted)	Wing mounted
Wing Specifications	AR	9.9
	Wing Span	64.9 ft (19.78 m)
	Wing area	424 sq. ft (39.4 sq.m)
Performance	Range	954 nm(1087 mi.,1750 km)
	Cruise speed	343 mph(298 knots,552km/h)
	Maximum Speed	378 mph (328 knots ,608 km/h)
	Takeoff Field Length	5118 ft (1560 m)
	Landing Field Length	4258 ft (1380 m)
	Stall speed	162 km/h (87 knots, 100 mph

Saab 340

		Saab 340
Purpose of Aircraft		Transport
W-0(Max Takeoff weight)		29,000 lbs (13,155 kg)
W-e (Empty weight)		19,000 lbs (8620 kg)
We/W0		0.66
Payload		Max=7,500 lb(3,400 kg)
Passengers(Total Weight of Passengers)		37+2
General dimensions	Length of aircraft	64.7 ft (19.73m)
	Height of aircraft	22.5 ft (6.87 m)
Engine(s)	Number	2
	Type(Turboprop)	General Electric CT7-9B
	power	1869 shp (1394 kW)
	Location(eg. Wing mounted)	Wing mounted
Wing Specifications	AR	10.9
	Wing Span	70.3 ft (21.44 m)
	Wing area	450 sq. ft(41.8 sq. m)
Performance	Range	910 nm.(1047 mi.,1685 km)
	Cruise speed	285.8 mph(248.38 knots,460 km/h)
	Maximum Speed	326 mph(283.477knots,525 km/h)
	Takeoff Field Length	4265ft (1300 m)
	Landing Field Length	3380 ft (1030 m)
	Stall speed	164 km/h (88 knots, 102 mph)

Beechcraft 1900D

		Beechcraft 1900D
Purpose of Aircraft		Transport
W-0(Max Takeoff weight)		17120 lbs(7766 kg)
W-e (Empty weight)		10590 lbs(4803 kg)
We/W0		0.62
Payload		Max.=5000lbs(2267.96kg)
Passengers(Total Weight of Passengers)		19+2
General dimensions	Length of aircraft	57.8 ft(17.62m)
	Height of aircraft	15.5ft(4.72m)
Engine(s)	Number	2
	Type(Turboprop)	Pratt & Whitney Canada PT6A-67D
	power	1279 shp(954 KW)
	Location(eg. Wing mounted)	Wing mounted
Wing Specifications	AR	10.8
	Wing Span	57.9ft(17.64m)
	Wing area	310 sq. ft(28.8 sq. m)
Performance	Range	1500 nm(1762 mi.,2778 km)
	Cruise speed	186.411mph(178knots3,00 km/h)
	Maximum Speed	285.209mph(248knots,459km/h)
	Takeoff Field Length	1140m(3740 ft)
	Landing Field Length	844m(2770ft)
	Stall speed	155.568 km/h(84 knots,96.6655mph)

British Aerospace Jetstream 41

		Bombadier Dash8Q100
Purpose of Aircraft		Transport
W-0(Max Takeoff weight)		36300lb(16470kg)
W-e (Empty weight)		23111lbs(10483kg)
We/W0		0.64
Payload		Max.=9038.95 lbs(4100kg)
Passengers(Total Weight of Passengers)		37+2
General dimensions	Length of aircraft	29ft 10in.(9.1m)
	Height of aircraft	8ft 10 in(2.69m)
Engine(s)	Number	2
	Type(Turboprop)	2 PW120A/PW121
	power	2000shp
	Location(eg. Wing mounted)	wing mounted
Wing Specifications	AR	12.3
	Wing Span	84ft 11 in.(25.89m)
	Wing area	585.55 sq. ft(54.4 sq.m)
Performance	Range	971.922nmi.(1118.47mi,1800km)
	Cruise speed	310 mph (269 knots,500 km/h)
	Maximum Speed	310.686mph(270 knots ,500 km/h)
	Takeoff Field Length	3,255 ft (992 m)
	Landing Field Length	2,580 ft (786 m)
	Stall speed	134km/h(72knots ,83mph)

APPENDIX B) MATLAB Code

Weight, Sizing, Geometry, Aerodynamics, Stability

```
clear,clc
%% Takeoff Weight Estimation using the methods described in Chapter 3 of
%% Aircraft Design: A Conceptual Approach by Daniel P. Raymer

% Copy of previously developed code re-written in all ENGLISH (fps) units
% for better consistency and to eliminate any unit errors that may or may
% not be present in other code

%% Defining the mission requirements

W_crew=360*2.2;       % [lb]
W_payload=3000*2.2;   % [lb]
Range1=700*6076.12;   % [ft] Regional Flight
Range2=100*6076.12;   % [ft] Divert

%%  Empty Weight Fraction, values from Table 3.1 in text

A=.96;     % English coefficient for twin turboprop
K_vs=1;    % Variable sweep constant, one for fixed sweep
C=-.05;    % Exponent for twin turboprop
fprintf('Sonata\n\n')
fprintf('============================================================\n\n')

% Fuel Fractions

% A) Warmup and takeoff, Climb, Landing

W1_W0=.97;    % Weight after warmup/takeoff over total gross weight
W2_W1=.985;   % Weight after climb over weight after takeoff
W5_W4=.995;   % Weight after landing over weight after loiter
W6_W5=.985;   % Weight after second climb over weight after landing attempt
W9_W8=.995;   % Weight after landing over weight after loiter

% B) Cruise Fuel Burn

C_crs_bhp=.44;  % [lb/hr/bhp] Table 3.4
V_knots=210;         % [knots]
V_fts=V_knots*1.688;
eta_pcrs=.8;   % Propeller efficiency for cruise
C_crs=C_crs_bhp*V_fts/(550*3600*eta_pcrs);

Swet_Sref=4.74;    % Taken from figure 3.6
AR_notips=10;   % Estimated from sketch, compared to similar configuration
AR=AR_notips*1.2;   % Effective Aspect Ratio with winglets
K_ld=11;        % Equation 3.12

L_Dmax_crs=K_ld*sqrt(AR./Swet_Sref);  % Equation 3.12, for cruise
```

```
W3_W2=exp(((-Range1*C_crs)./(V_fts*L_Dmax_crs))); % From range equation
W7_W6=exp(((-Range2*C_crs)./(V_fts*L_Dmax_crs))); % From range equation

% C) Loiter Fuel Burn

L_Dmax_lot=L_Dmax_crs*.866;    % Most efficient L/D for loiter
E=2700;           % [s] Loiter time for IFR
C_bhp_lot=.55;     % [lb/hr/bhp] Specific Fuel Consumption of turboprop from
Table 3.4
eta_plot=.7;
C_lot=C_bhp_lot*V_fts/(3600*550*eta_plot);

W4_W3=exp((-E*C_lot)./L_Dmax_lot);  % From Endurance equation
W8_W7=exp((-E*C_lot)./L_Dmax_lot);  % From Endurance equation

% D) Overall Fuel Fraction

Wx_W0=W9_W8.*W8_W7.*W7_W6.*W6_W5.*W5_W4.*W4_W3.*W3_W2.*W2_W1.*W1_W0;

Wf_W0=1.06*(1-Wx_W0);  % Total fuel fraction assuming 6% trapped in tanks

% Iterative Takeoff Weight Calculation

n=0;  % Initializing iteration counter
W_0est=30000;
W_0calc=0;  % Initializing W_0calc for first comparison

while abs(W_0est-W_0calc)>1;

    n=n+1;
    We_W0=A*(W_0est.^C)*K_vs;
    W_0calc=.95*(W_crew+W_payload)./(1-Wf_W0-We_W0);  % .95 for composites
    W_0est=W_0est+(W_0calc-W_0est)*.75;

end

Wf=Wf_W0.*W_0calc;
We=We_W0.*W_0calc;
fprintf('Values derived during intitial weight analysis \n\n\n')
fprintf('Max Takeoff Weight: %.0f lbs \n\n',W_0calc)
fprintf('Max Fuel Capacity: %.0f lbs \n\n',Wf)
fprintf('Empty Weight: %.0f lbs \n\n',We)
fprintf('Empty Weight Fraction: %.3f \n\n',We_W0)
fprintf('Fuel Fraction: %.3f \n\n',Wf_W0)
fprintf('Max L/D during cruise: %.2f \n\n',L_Dmax_crs)
fprintf('Max L/D during loiter: %.2f \n\n',L_Dmax_lot)
fprintf('============================================================\n\n')

%% Power Loading and Wing Loading

% Thrust to Weight Ratio or Power Loading
```

```
fprintf('Values derived for Thrust/Power Loading and Wing Loading\n\n\n')

alpha=.013;             % Power to weight ratio constants from Table 5.4
c=.5;
P_W0=(alpha*V_knots^c);         % Equation from Table 5.4
T_W0=(eta_plot*550/(V_fts))*P_W0;   % Finding thrust to weight ratio for prop
fprintf('Power to Weight Ratio: %.3f hp/lb\n\n',P_W0)
fprintf('Thrust to Weight Ratio: %.3f \n\n',T_W0)

T_W_OEI=T_W0/2;   % Thrust to weight ratio for OEI
P_W_OEI=P_W0/2;

T_W0_crs=1./L_Dmax_crs;
fprintf('Thrust to Weight Ratio for cruise: %.3f \n\n',T_W0_crs)
T_W0_crs_match=T_W0_crs*(W1_W0*W2_W1)/.6;

T_W0_climb=1/(L_Dmax_crs*.8)+.03;
T_W0_climb_match=T_W0_climb*(W1_W0)/.8;

fprintf('Thrust to Weight Ratio for cruise (matched): %.3f \n\n',...
    T_W0_crs_match)
fprintf('Thrust to Weight Ratio for climb (matched): %.3f \n\n',...
    T_W0_climb_match)

% Wing Loading

% Stall Wing Loading

rho_actual=18.82E-4;    % [slug/ft^3] Denver Air density in summer
rho_SL=23.77E-4;        % [slug/ft^3] Sea-level air density
S_ref=700;          % [ft^2] Wing reference area
S_fl=S_ref*.6;          % [ft^2] Wing reference area with flaps
S_unfl=S_ref*.4;        % [ft^2] Wing reference area without flaps
C_l_max_unfl=1.8;   % Airfoil max lift coefficient with no high lift devices
C_l_max_fl=2.8;
Quarter_c_sweep=8;      % Quarter chord sweep in degrees
Leading_sweep=10;       % Leading edge sweep in degrees
V_stall=130;
C_L_max=.9*(C_l_max_fl*(S_fl/S_ref)+C_l_max_unfl*(S_unfl/S_ref))*...
    cos(Quarter_c_sweep*pi()/180);
fprintf('Max Lift Coefficient: %.2f \n\n',C_L_max)
W_S_stall=.5*rho_actual*V_stall^2*C_L_max;
fprintf('Wing Loading for Stall: <= %.2f lb/ft^2 \n\n',W_S_stall)

% Takeoff Wing Loading (1000m)

sigma=rho_actual/rho_SL;  % Air density ratio (1 at sea level)
C_L_TO=C_L_max/1.1^2;
fprintf('Takeoff Lift Coefficient: %.2f \n\n',C_L_TO)

TOP_1000=400;   % Approximated from Fig 5.4
W_S_takeoff_TOP=TOP_1000*sigma*C_L_TO*P_W0;
W_S_takeoff_OEI=TOP_1000*sigma*C_L_TO*P_W_OEI;
```

```
fprintf('Wing Loading for Takeoff (1000m): %.2f lb/ft^2 \n\n'...
    ,W_S_takeoff_TOP);
fprintf('Wing Loading for Takeoff with OEI (1000m): %.2f lb/ft^2 \n\n'...
    ,W_S_takeoff_OEI);

% Actual Takeoff Distance

e=1.78*(1-.045*AR.^.68)-.64;

if (Leading_sweep>30)
    e=4.61*(1-.045*AR^.68)*(cos(Leading_sweep*pi()/180))^.15-3.1; %Eq 12.49
end
K=1./(pi()*e.*AR);

mu_TO=.05;      % Rolling, dry concrete (.02 for icy concrete)
V_TO=1.1*V_stall;
C_f_e=.0026;    % Civil Transport taken from Table 12.3
C_D_0=C_f_e*Swet_Sref;  % Approximation from Fig 12.34

C_D_TO=C_D_0+.02+K*C_L_TO^2;    % Drag Coefficient buildup for takeoff
                                    % corrected for flaps (C_D_0+.02)

K_T=T_W0-mu_TO;
K_A=(rho_actual/2)*(1./W_S_stall).*(mu_TO*C_L_TO-C_D_TO);
S_g=1./(2*32.174*K_A).*log(1+(K_A/K_T).*V_TO.^2);

h_OB=35;        % [ft] Obstacle height (35ft) as described in FAR25.101
V_TR=1.15*V_stall;  % [ft/s] Transition Velocity from TO to Climb
V_climb=1.21*V_stall;   % [ft/s]  Climb speed during takeoff segment
Radius_TO=V_TR.^2/(.2*32.174);  % Takeoff radius eq 17.107
S_TR=sqrt(Radius_TO.^2-(Radius_TO-h_OB).^2);% Transition distance eq 17.111

S_total=S_g+S_TR;  % [m] Total takeoff distance per FAR25.113

fprintf('Takeoff Ground Roll: %.0f ft \n\n',S_g)
fprintf('Takeoff Transition Distance: %.0f ft \n\n',S_TR)
fprintf('Total Takeoff Distance: %.0f ft \n\n',S_total)

% Landing Wing Loading

S_a=1000;           % [ft] taken from p.133
S_landing=3000;     % [ft] Bombardier Dash 8 landing distance for comparison

W_S_landing=(S_landing-S_a)*sigma*C_L_max/80*1.67;  % Corrected for
                                                    % safety/gravity
fprintf('Wing Loading for Landing: %.2f lb/ft^2 \n\n',W_S_landing)

% Wing Loading for max range

W_S_cruise=.5*rho_actual*V_fts.^2*sqrt(3*pi()*AR.*e*C_D_0).*(.97*.985);
```

```
fprintf('Wing Loading for Max Range Cruise: %.2f lb/ft^2 \n\n',W_S_cruise)

W_S=min([W_S_cruise,W_S_landing,W_S_stall,W_S_takeoff_TOP,...
    W_S_takeoff_OEI]);

fprintf('Selected Wing Loading: %.2f lb/ft^2 \n\n',W_S)

T_W0_min=.03+2*sqrt((C_D_0+.02)/(pi()*AR*e*.95));
T_W_stall=W_S/(C_L_TO*sigma*TOP_1000);

T_W=max([T_W0,T_W_stall,T_W0_min]);
fprintf('Selected Thrust to Weight Ratio: %.3f \n\n',T_W)

%% Refined Sizing Method
fprintf('============================================================\n\n')
fprintf('Refined Sizing Results\n\n\n')

W_0est=30000;
while abs(W_0est-W_0calc)>1;

We_W0=.37+.09*(W_0est^-.06)*(AR^.08)*(P_W0^.08)*(W_S^-.05)*...
    ((V_knots)^.3);

W1_W0=.97;
W2_W1=1.0065-.0325*(V_fts/1234.99);
W5_W4=.995;
W6_W5=W2_W1;
W9_W8=.997;

rho_cruise=10.66E-4;
L_D_crs=((.5*rho_cruise*V_fts^2*C_D_0)/W_S+W_S*(.5*...
    rho_cruise*V_fts^2*pi()*AR*e)^-1)^-1;
W3_W2=exp(((-Range1*C_crs)./(V_fts*L_D_crs))); % From range equation
W7_W6=exp(((-Range2*C_crs)./(V_fts*L_D_crs))); % From range equation

Wf1=(1-W1_W0)*W_0est;
Wf2=(1-W2_W1)*(W_0est-Wf1);
Wf3=(1-W3_W2)*(W_0est-Wf2-Wf1);
Wf4=(1-W4_W3)*(W_0est-Wf3-Wf2-Wf1);
Wf5=(1-W5_W4)*(W_0est-Wf4-Wf3-Wf2-Wf1);
Wf6=(1-W6_W5)*(W_0est-Wf5-Wf4-Wf3-Wf2-Wf1);
Wf7=(1-W7_W6)*(W_0est-Wf6-Wf5-Wf4-Wf3-Wf2-Wf1);
Wf8=(1-W8_W7)*(W_0est-Wf7-Wf6-Wf5-Wf4-Wf3-Wf2-Wf1);
Wf9=(1-W9_W8)*(W_0est-Wf8-Wf7-Wf6-Wf5-Wf4-Wf3-Wf2-Wf1);

Wf=1.06*(Wf1+Wf2+Wf3+Wf4+Wf5+Wf6+Wf7+Wf8+Wf9);

W_0calc=W_crew+W_payload+Wf+We_W0*W_0est;

W_0est=W_0est+(W_0calc-W_0est)*.75;
end
```

```
P_engine=2940;
N=2;
P_W0=P_engine*N/(W_0calc);
T_W0=(eta_plot*550/(V_fts))*P_W0;
Wf_W0=Wf/W_0calc;
We=We_W0*W_0calc;
S_ref=W_0calc/W_S;
W_S=W_0calc/S_ref;

fprintf('Max Takeoff Weight: %.0f lb \n\n',W_0calc)
fprintf('Empty Weight: %.0f lb \n\n',We)
fprintf('Max Fuel Capacity: %.0f lb \n\n',Wf)
fprintf('Empty Weight Fraction: %.3f \n\n',We_W0)
fprintf('Fuel Fraction: %.3f \n\n',Wf_W0)
fprintf('Power to Weight Ratio: %.3f hp/lb \n\n',P_W0)
fprintf('Thrust to Weight Ratio: %.3f \n\n',T_W0)
fprintf('Wing Loading: %.2f lb/ft^2\n\n',W_S)
fprintf('Wing Reference Area: %.1f ft^2\n\n',S_ref)

%% Geometric Calculations
fprintf('=============================================================\n\n')
fprintf('Geometric Calculations\n\n\n')

lambda=.614;
c_VT=.08;
c_HT=.9;
l_fuse=81;
l_VT=.55*l_fuse;
l_HT=.55*l_fuse;
b=sqrt(AR*S_ref);
C_root=2*S_ref/(b*(1+lambda));
C_tip=lambda*C_root;
C_bar=2/3*C_root*(1+lambda+lambda^2)/(1+lambda);
y_bar=b/6*(1+2*lambda)/(1+lambda);
x=(1+2*lambda)/12*C_root*AR*tan(Leading_sweep*pi()/180);
x_bar=x+.25*C_bar;
S_vert=c_VT*b*S_ref/l_VT;
S_horz=c_HT*C_bar*S_ref/l_HT;

fprintf('Wing Span: %.1f ft\n\n',b)
fprintf('Root Chord: %.1f ft\n\n',C_root)
fprintf('Tip Chord: %.1f ft\n\n',C_tip)
fprintf('Mean Aerodynamic Chord: %.1f ft\n\n',C_bar)
fprintf('Span Location of MAC: %.1f ft\n\n',y_bar)
fprintf('Leading Edge of MAC (relative to root LE): %.1f ft\n\n',x)
fprintf('Aerodynamic Center of MAC (relative to root LE): %.1f ft\n',x_bar)
fprintf('\nVertical Tail Area: %.1f ft^2\n\n',S_vert);
fprintf('Horizontal Tail Area: %.1f ft^2\n\n',S_horz);

%% Validating Wetted Area Ratio
fprintf('=============================================================\n\n')
fprintf('Wetted Area Calculations (Post-sizing)\n\n\n')

S_expW=.8*S_ref;
```

```
A_topfuse=572;
A_sidefuse=543.6;
t_c_W=.15;
t_c_T=.1;
S_wetW=S_expW*(1.977+.52*t_c_W);
S_wetVT=S_vert*(1.977+.52*t_c_T);
S_wetHT=S_horz*(1.977+.52*t_c_T);
S_wetFuse=3.4*(A_topfuse+A_sidefuse)/2;
S_wetEng=140;
S_wet=S_wetW+S_wetVT+S_wetHT+S_wetFuse+S_wetEng;
Swet_Sref=S_wet/S_ref;

fprintf('Wing Wetted Area: %.0f ft^2\n\n',S_wetW)
fprintf('VT Wetted Area: %.0f ft^2\n\n',S_wetVT)
fprintf('HT Wetted Area: %.0f ft^2\n\n',S_wetHT)
fprintf('Fuselage Wetted Area: %.0f ft^2\n\n',S_wetFuse)
fprintf('Engine Wetted Area: %.0f ft^2\n\n',S_wetEng)
fprintf('New Wetted Area Ratio: %.2f\n\n',Swet_Sref)

%% Detailed Weights Analysis
fprintf('================================================================\n\n')
fprintf('Weight Breakdown \n\n\n')

lambda=.614;
Lambda=Quarter_c_sweep;
Lambda_ht=0;
Lambda_vt=30;
L=80;
L_t=48.4;
AR=13.2;
AR_h=7.23;
AR_v=1.9;
B_h=33;
B_w=108.4;
D=.5;
D_e=3.33;
F_w=6.5;
H_t=0;
Ht_Hv=0;
H_v=18;
I_yaw=327504;
K_cb=1;
K_d=1.68;
K_door=1.06;
K_dw=1;
K_dwf=1;
K_h=.11;
K_Lg=1;
K_mc=1;
K_mp=1;
K_ng=1;
K_np=1;
K_p=1.4;
K_r=1;
```

```
K_rht=1;
K_tp=.793;
K_tpg=1;
K_tr=1;
K_uht=1;
K_vg=1;
K_vs=1;
K_vsh=1;
K_ws=.75*((1+2*lambda)/(1+lambda))*(B_w*tan(Lambda*pi/180/L));
K_y=.3*L_t;
K_z=L_t;
L_a=60;
L_ec=40;
L_f=l_fuse;
L_m=84;
L_n=84;
N_c=4;
N_ci=2;
N_en=2;
N_f=7;
N_gen=2;
N_Lt=9;
N_l=4.5;
N_m=2;
N_mss=2;
N_mw=4;
N_p=39;
N_t=3;
N_u=15;
N_w=3.33;
N_z=4.5;
R_kva=60;
S_cs=240.8;
S_csw=178.12;
S_e=28;
S_f=S_wetFuse;
S_ht=S_horz;
S_n=S_wetEng;
S_r=34.68;
S_stall=77;
S_vt=S_vert;
S_w=S_ref;
t_c=.15;
V_t=724.3;
V_i=.5*V_t;
V_p=V_t-V_i;
V_pr=2309.1;
W_c=7700;
W_dg=W_0calc;
W_en=1064;
W_ec=2.331*(W_en^.901)*K_p*K_tr;
W_l=W_0calc*.95;
W_press=11.9*(V_pr*8)^.271;
W_uav=800;
```

```
W_wing=.85*(.0051*(W_dg*N_z)^.557*S_w^.649*AR^.5*t_c^-
.4*(1+lambda)^.1*(cos(Lambda*pi/180))^-1*S_csw^.1);
W_HT=.83*(.0379*K_uht*(1+F_w/B_h)^-.25*W_dg^.639*N_z^.1*S_ht^.75*L_t^-
1*K_y^.704*(cos(Lambda_ht*pi/180))^-1*AR_h^.166*(1+S_e/S_ht)^.1);
W_VT=.83*(.0026*(1+Ht_Hv)^.225*W_dg^.556*N_z^.536*L_t^-
.5*S_vt^.5*K_z^.875*(cos(Lambda_vt*pi/180))^-1*AR_v^.35*t_c^-.5);
W_fuse=.9*(.328*K_door*K_Lg*(W_dg*N_z)^.5*L^.25*S_f^.302*(1+K_ws)^.04*(L_D_cr
s)^.1);
W_MLG=.95*(.0106*K_mp*W_l^.888*N_l^.25*L_m^.4*N_mw^.321*N_mss^-
.5*V_stall^.1);
W_NLG=.95*(.032*K_np*W_l^.646*N_l^.2*L_n^.5*N_mw^.45);
W_nacelle=.9*(.6724*K_ng*N_Lt^.1*N_w^.294*N_z^.119*W_ec^.611*N_en^.984*S_n^.2
24);
W_engcon=5*N_en+.8*L_ec;
W_start=49.19*(N_en*W_en/1000)^.541;
W_fuelsys=2.405*V_t^.606*(1+V_i/V_t)^-1*(1+V_p/V_t)*N_t^.5;
W_flightcon=145.9*N_f^.554*(1+N_m/N_f)^-1*S_cs^.2*(I_yaw*10^-6)^.07;
W_APU=524;
W_instru=4.509*K_r*K_tp*N_c^.541*N_en*(L_f+B_w)^.5;
W_hydro=.2673*N_f*(L_f+B_w)^.937;
W_elec=7.291*R_kva^.782*L_a^.346*N_gen^.1;
W_avion=1.73*W_uav^.983;
W_furn=.0577*N_c^.1*W_c^.393*S_f^.75;
W_AC=62.36*N_p^.25*(V_pr/1000)^.604*W_uav^.1;
W_antiice=.002*W_dg*N_gen^.1;
W_engine=2128;
W_passseats=32*37;
W_pilotseats=2*60;
W_lavatory=.31*35^1.33;

W_structure=W_wing+W_HT+W_VT+W_fuse+W_MLG+W_NLG+W_nacelle;
W_prop=W_engine+W_engcon+W_start+W_fuelsys;
W_equip=W_flightcon+W_APU+W_instru+W_hydro+W_elec+W_avion+W_furn+W_AC+W_antii
ce+W_passseats+W_pilotseats+W_lavatory;

W_empty=W_structure+W_prop+W_equip;
W_usable=W_0calc-W_empty;
W_fuel=W_usable-W_payload-W_crew;

fprintf('Wing - %.0f lbs\n',W_wing)
fprintf('Horizontal Tail - %.0f lbs\n',W_HT)
fprintf('Vertical Tail - %.0f lbs\n',W_VT)
fprintf('Fuselage - %.0f lbs\n',W_fuse)
fprintf('Main Gear - %.0f lbs\n',W_MLG)
fprintf('Nose Gear - %.0f lbs\n',W_NLG)
fprintf('Nacelle - %.0f lbs\n',W_nacelle)
fprintf('Engine Controls - %.0f lbs\n',W_engcon)
fprintf('Starter - %.0f lbs\n',W_start)
fprintf('Fuel System - %.0f lbs\n',W_fuelsys)
fprintf('Flight Controls - %.0f lbs\n',W_flightcon)
fprintf('APU - %.0f lbs\n',W_APU)
fprintf('Instruments - %.0f lbs\n',W_instru)
fprintf('Hydraulics - %.0f lbs\n',W_hydro)
fprintf('Electronics - %.0f lbs\n',W_elec)
```

```
fprintf('Avionics - %.0f lbs\n',W_avion)
fprintf('Furnishings - %.0f lbs\n',W_furn)
fprintf('Air Conditioning - %.0f lbs\n',W_AC)
fprintf('Anti-Ice - %.0f lbs\n',W_antiice)
fprintf('Engines - %.0f lbs\n',W_engine)
fprintf('Passenger Seats - %.0f lbs\n',W_passseats)
fprintf('Pilot Seats - %.0f lbs\n\n',W_pilotseats)
fprintf('Structural Weight - %.0f lbs\n',W_structure)
fprintf('Propulsion Weight - %.0f lbs\n',W_prop)
fprintf('Equipment Weight - %.0f lbs\n\n',W_equip)
fprintf('New Empty Weight - %.0f lbs\n',W_empty)
fprintf('Usable Weight - %.0f lbs\n',W_usable)
fprintf('Weight left for Fuel - %.0f lbs\n\n',W_fuel)

%% Weight Approximations (again)
fprintf('============================================================\n\n')
fprintf('Weight Approximations (again)\n\n\n')

W_02=W_empty+Wf+W_payload+W_crew;
W_e2=W_empty*(W_02/W_0calc)^.9;

W_0calc=W_e2+Wf+W_payload+W_crew;
while abs(W_0est-W_0calc)>1;

We_W0=W_e2/W_0calc;

W1_W0=.97;
W2_W1=1.0065-.0325*(V_fts/1234.99);
W5_W4=.995;
W6_W5=W2_W1;
W9_W8=.997;

rho_cruise=10.66E-4;
L_D_crs=((.5*rho_cruise*V_fts^2*C_D_0)/W_S+W_S*(.5*...
    rho_cruise*V_fts^2*pi()*AR*e)^-1)^-1;
W3_W2=exp(((-Range1*C_crs)./(V_fts*L_D_crs))); % From range equation
W7_W6=exp(((-Range2*C_crs)./(V_fts*L_D_crs))); % From range equation

Wf1=(1-W1_W0)*W_0est;
Wf2=(1-W2_W1)*(W_0est-Wf1);
Wf3=(1-W3_W2)*(W_0est-Wf2-Wf1);
Wf4=(1-W4_W3)*(W_0est-Wf3-Wf2-Wf1);
Wf5=(1-W5_W4)*(W_0est-Wf4-Wf3-Wf2-Wf1);
Wf6=(1-W6_W5)*(W_0est-Wf5-Wf4-Wf3-Wf2-Wf1);
Wf7=(1-W7_W6)*(W_0est-Wf6-Wf5-Wf4-Wf3-Wf2-Wf1);
Wf8=(1-W8_W7)*(W_0est-Wf7-Wf6-Wf5-Wf4-Wf3-Wf2-Wf1);
Wf9=(1-W9_W8)*(W_0est-Wf8-Wf7-Wf6-Wf5-Wf4-Wf3-Wf2-Wf1);

Wf=1.06*(Wf1+Wf2+Wf3+Wf4+Wf5+Wf6+Wf7+Wf8+Wf9);

W_0calc=W_crew+W_payload+Wf+We_W0*W_0est;

W_0est=W_0est+(W_0calc-W_0est)*.75;
```

```
end

P_engine=2940;
N=2;
P_W0=P_engine*N/(W_0calc);
T_W0=(eta_plot*550/(V_fts))*P_W0;
Wf_W0=Wf/W_0calc;
We=We_W0*W_0calc;
S_ref=W_0calc/W_S;
W_S=W_0calc/S_ref;

fprintf('Max Takeoff Weight: %.0f lb \n\n',W_0calc)
fprintf('Empty Weight: %.0f lb \n\n',We)
fprintf('Max Fuel Capacity: %.0f lb \n\n',Wf)
fprintf('Empty Weight Fraction: %.3f \n\n',We_W0)
fprintf('Fuel Fraction: %.3f \n\n',Wf_W0)
fprintf('Power to Weight Ratio: %.3f hp/lb \n\n',P_W0)
fprintf('Thrust to Weight Ratio: %.3f \n\n',T_W0)
fprintf('Wing Loading: %.2f lb/ft^2\n\n',W_S)
fprintf('Wing Reference Area: %.1f ft^2\n\n',S_ref)

%% Geometric Calculations 2
fprintf('============================================================\n\n')
fprintf('Geometric Calculations 2\n\n\n')

lambda=.614;
c_VT=.08;
c_HT=.9;
l_fuse=88.3;
l_VT=.55*l_fuse;
l_HT=.55*l_fuse;
b=sqrt(AR_notips*S_ref);
C_root=2*S_ref/(b*(1+lambda));
C_tip=lambda*C_root;
C_bar=2/3*C_root*(1+lambda+lambda^2)/(1+lambda);
y_bar=b/6*(1+2*lambda)/(1+lambda);
x=(1+2*lambda)/12*C_root*AR*tan(Leading_sweep*pi()/180);
x_bar=x+.25*C_bar;
S_vert=c_VT*b*S_ref/l_VT;
S_horz=c_HT*C_bar*S_ref/l_HT;

fprintf('Wing Span: %.1f ft\n\n',b)
fprintf('Root Chord: %.1f ft\n\n',C_root)
fprintf('Tip Chord: %.1f ft\n\n',C_tip)
fprintf('Mean Aerodynamic Chord: %.1f ft\n\n',C_bar)
fprintf('Span Location of MAC: %.1f ft\n\n',y_bar)
fprintf('Leading Edge of MAC (relative to root LE): %.1f ft\n\n',x)
fprintf('Aerodynamic Center of MAC (relative to root LE): %.1f ft\n',x_bar)
fprintf('\nVertical Tail Area: %.1f ft^2\n\n',S_vert);
fprintf('Horizontal Tail Area: %.1f ft^2\n\n',S_horz);

%% Validating Wetted Area Ratio 2
fprintf('============================================================\n\n')
fprintf('Wetted Area Calculations 2 (Post-sizing)\n\n\n')
```

```
S_expW=.8*S_ref;
A_topfuse=572;
A_sidefuse=543.6;
t_c_W=.15;
t_c_T=.1;
S_wetW=S_expW*(1.977+.52*t_c_W);
S_wetVT=S_vert*(1.977+.52*t_c_T);
S_wetHT=S_horz*(1.977+.52*t_c_T);
S_wetFuse=3.4*(A_topfuse+A_sidefuse)/2;
S_wetEng=140;
S_wet=S_wetW+S_wetVT+S_wetHT+S_wetFuse+S_wetEng;
Swet_Sref=S_wet/S_ref;

fprintf('Wing Wetted Area: %.0f ft^2\n\n',S_wetW)
fprintf('VT Wetted Area: %.0f ft^2\n\n',S_wetVT)
fprintf('HT Wetted Area: %.0f ft^2\n\n',S_wetHT)
fprintf('Fuselage Wetted Area: %.0f ft^2\n\n',S_wetFuse)
fprintf('Engine Wetted Area: %.0f ft^2\n\n',S_wetEng)
fprintf('New Wetted Area Ratio: %.2f\n\n',Swet_Sref)

%% Detailed Weights Analysis 2
fprintf('============================================================\n\n')
fprintf('Weight Breakdown 2\n\n\n')

lambda=.614;
Lambda=Quarter_c_sweep;
Lambda_ht=0;
Lambda_vt=30;
L=80;
L_t=l_fuse*.6;
AR=13.2;
AR_h=7.23;
AR_v=1.9;
B_h=33;
B_w=108.4;
D=.5;
D_e=3.33;
F_w=6.5;
H_t=0;
Ht_Hv=0;
H_v=18;
I_yaw=327504;
K_cb=1;
K_d=1.68;
K_door=1.06;
K_dw=1;
K_dwf=1;
K_h=.11;
K_Lg=1;
K_mc=1;
K_mp=1;
K_ng=1;
K_np=1;
```

```
K_p=1.4;
K_r=1;
K_rht=1;
K_tp=.793;
K_tpg=1;
K_tr=1;
K_uht=1;
K_vg=1;
K_vs=1;
K_vsh=1;
K_ws=.75*((1+2*lambda)/(1+lambda))*(B_w*tan(Lambda*pi/180/L));
K_y=.3*L_t;
K_z=L_t;
L_a=60;
L_ec=40;
L_f=l_fuse;
L_m=84;
L_n=84;
N_c=4;
N_ci=2;
N_en=2;
N_f=7;
N_gen=2;
N_Lt=9;
N_l=4.5;
N_m=2;
N_mss=2;
N_mw=4;
N_p=39;
N_t=3;
N_u=15;
N_w=3.33;
N_z=4.5;
R_kva=60;
S_cs=240.8;
S_csw=178.12;
S_e=28;
S_f=S_wetFuse;
S_ht=S_horz;
S_n=S_wetEng;
S_r=34.68;
S_stall=77;
S_vt=S_vert;
S_w=S_ref;
t_c=.15;
V_t=724.3;
V_i=.5*V_t;
V_p=V_t-V_i;
V_pr=2309.1;
W_c=7700;
W_dg=W_0calc;
W_en=1064;
W_ec=2.331*(W_en^.901)*K_p*K_tr;
W_l=W_0calc*.95;
W_press=11.9*(V_pr*8)^.271;
```

```
W_uav=800;

W_wing=.85*(.0051*(W_dg*N_z)^.557*S_w^.649*AR^.5*t_c^-
.4*(1+lambda)^.1*(cos(Lambda*pi/180))^-1*S_csw^.1);
W_HT=.83*(.0379*K_uht*(1+F_w/B_h)^-.25*W_dg^.639*N_z^.1*S_ht^.75*L_t^-
1*K_y^.704*(cos(Lambda_ht*pi/180))^-1*AR_h^.166*(1+S_e/S_ht)^.1);
W_VT=.83*(.0026*(1+Ht_Hv)^.225*W_dg^.556*N_z^.536*L_t^-
.5*S_vt^.5*K_z^.875*(cos(Lambda_vt*pi/180))^-1*AR_v^.35*t_c^-.5);
W_fuse=.9*(.328*K_door*K_Lg*(W_dg*N_z)^.5*L^.25*S_f^.302*(1+K_ws)^.04*(L_D_cr
s)^.1);
W_MLG=.95*(.0106*K_mp*W_l^.888*N_l^.25*L_m^.4*N_mw^.321*N_mss^-
.5*V_stall^.1);
W_NLG=.95*(.032*K_np*W_l^.646*N_l^.2*L_n^.5*N_mw^.45);
W_nacelle=.9*(.6724*K_ng*N_Lt^.1*N_w^.294*N_z^.119*W_ec^.611*N_en^.984*S_n^.2
24);
W_engcon=5*N_en+.8*L_ec;
W_start=49.19*(N_en*W_en/1000)^.541;
W_fuelsys=2.405*V_t^.606*(1+V_i/V_t)^-1*(1+V_p/V_t)*N_t^.5;
W_flightcon=145.9*N_f^.554*(1+N_m/N_f)^-1*S_cs^.2*(I_yaw*10^-6)^.07;
W_APU=524;
W_instru=4.509*K_r*K_tp*N_c^.541*N_en*(L_f+B_w)^.5;
W_hydro=.2673*N_f*(L_f+B_w)^.937;
W_elec=7.291*R_kva^.782*L_a^.346*N_gen^.1;
W_avion=1.73*W_uav^.983;3953.5;
W_furn=.0577*N_c^.1*W_c^.393*S_f^.75;
W_AC=62.36*N_p^.25*(V_pr/1000)^.604*W_uav^.1;
W_antiice=.002*W_dg*N_gen^.1;
W_engine=2128;
W_passseats=32*37;
W_pilotseats=2*60;
W_lavatory=.31*35^1.33;

W_structure=W_wing+W_HT+W_VT+W_fuse+W_MLG+W_NLG+W_nacelle;
W_prop=W_engine+W_engcon+W_start+W_fuelsys;
W_equip=W_flightcon+W_APU+W_instru+W_hydro+W_elec+W_avion+W_furn+W_AC+W_antii
ce+W_passseats+W_pilotseats+W_lavatory;

W_empty=W_structure+W_prop+W_equip;
W_usable=W_0calc-W_empty;
W_fuel=W_usable-W_payload-W_crew;

fprintf('Wing - %.0f lbs\n',W_wing)
fprintf('Horizontal Tail - %.0f lbs\n',W_HT)
fprintf('Vertical Tail - %.0f lbs\n',W_VT)
fprintf('Fuselage - %.0f lbs\n',W_fuse)
fprintf('Main Gear - %.0f lbs\n',W_MLG)
fprintf('Nose Gear - %.0f lbs\n',W_NLG)
fprintf('Nacelle - %.0f lbs\n',W_nacelle)
fprintf('Engine Controls - %.0f lbs\n',W_engcon)
fprintf('Starter - %.0f lbs\n',W_start)
fprintf('Fuel System - %.0f lbs\n',W_fuelsys)
fprintf('Flight Controls - %.0f lbs\n',W_flightcon)
fprintf('APU - %.0f lbs\n',W_APU)
fprintf('Instruments - %.0f lbs\n',W_instru)
```

```
fprintf('Hydraulics - %.0f lbs\n',W_hydro)
fprintf('Electronics - %.0f lbs\n',W_elec)
fprintf('Avionics - %.0f lbs\n',W_avion)
fprintf('Furnishings - %.0f lbs\n',W_furn)
fprintf('Air Conditioning - %.0f lbs\n',W_AC)
fprintf('Anti-Ice - %.0f lbs\n',W_antiice)
fprintf('Engines - %.0f lbs\n',W_engine)
fprintf('Passenger Seats - %.0f lbs\n',W_passseats)
fprintf('Pilot Seats - %.0f lbs\n',W_pilotseats)
fprintf('Lavatory - %.0f lbs\n\n',W_lavatory)
fprintf('Structural Weight - %.0f lbs\n',W_structure)
fprintf('Propulsion Weight - %.0f lbs\n',W_prop)
fprintf('Equipment Weight - %.0f lbs\n\n',W_equip)
fprintf('New Empty Weight - %.0f lbs\n',W_empty)
fprintf('Usable Weight - %.0f lbs\n',W_usable)
fprintf('Weight left for Fuel - %.0f lbs\n\n',W_fuel)

%% Checking Takeoff Distance
fprintf('============================================================\n\n')
fprintf('Takeoff Distance 2\n\n\n')


C_D_0=C_f_e*Swet_Sref;  % Approximation from Fig 12.34

C_D_TO=C_D_0+.02+K*C_L_TO^2;  % Drag Coefficient buildup for takeoff
                                                    % corrected for flaps
(C_D_0+.02)

K_T=T_W0-mu_TO;
K_A=(rho_actual/2)*(1./W_S_stall).*(mu_TO*C_L_TO-C_D_TO);
S_g=1./(2*32.174*K_A).*log(1+(K_A/K_T).*V_TO.^2);

h_OB=35;   % [m] Obstacle height (35ft) as described in FAR25.101
V_TR=1.15*V_stall;  % [m/s] Transition Velocity from TO to Climb
V_climb=1.21*V_stall;  % [m/s]  Climb speed during takeoff segment
Radius_TO=V_TR.^2/(.2*32.174);  % Takeoff radius eq 17.107
S_TR=sqrt(Radius_TO.^2-(Radius_TO-h_OB).^2);% Transition distance eq 17.111

S_total=S_g+S_TR;  % [m] Total takeoff distance per FAR25.113

fprintf('Takeoff Ground Roll: %.0f ft \n\n',S_g)
fprintf('Takeoff Transition Distance: %.0f ft \n\n',S_TR)
fprintf('Total Takeoff Distance: %.0f ft \n\n',S_total)
L_Dmaxcrs=K_ld*sqrt(AR/Swet_Sref);

%% Checking Zero-Lift Drag
fprintf('============================================================\n\n')
fprintf('Zero-Lift Drag Buildup\n\n\n')

M=.358;
dyn_visc=3.324E-7;
Rey_fuse_crs=rho_cruise*V_fts*l_fuse/dyn_visc;
Rey_fuse_TO=rho_cruise*V_stall*1.1*l_fuse/dyn_visc;
```

```
Rey_nac_crs=rho_cruise*V_fts*12/dyn_visc;
Rey_nac_TO=rho_cruise*V_stall*1.1*12/dyn_visc;
Rey_wing_crs=rho_cruise*V_fts*C_bar/dyn_visc;
Rey_wing_TO=rho_cruise*V_stall*1.1*C_bar/dyn_visc;
Rey_VT_crs=rho_cruise*V_fts*10/dyn_visc;
Rey_VT_TO=rho_cruise*V_stall*1.1*10/dyn_visc;
Rey_HT_crs=rho_cruise*V_fts*5.82/dyn_visc;
Rey_HT_TO=rho_cruise*V_stall*1.1*5.82/dyn_visc;


Cf_fuselam=1.328/sqrt(Rey_fuse_crs);
Cf_fusetur=.455/(log10(Rey_fuse_crs))^2.58;
Cf_fuse_crs=.1*Cf_fuselam+.9*Cf_fusetur;
Cf_fuselam=1.328/sqrt(Rey_fuse_TO);
Cf_fusetur=.455/(log10(Rey_fuse_TO))^2.58;
Cf_fuse_TO=.1*Cf_fuselam+.9*Cf_fusetur;

Cf_naclam=1.328/sqrt(Rey_nac_crs);
Cf_nactur=.455/(log10(Rey_nac_crs))^2.58;
Cf_nacelle_crs=.1*Cf_naclam+.9*Cf_nactur;
Cf_naclam=1.328/sqrt(Rey_nac_TO);
Cf_nactur=.455/(log10(Rey_nac_TO))^2.58;
Cf_nacelle_TO=.1*Cf_naclam+.9*Cf_nactur;

Cf_winglam=1.328/sqrt(Rey_wing_crs);
Cf_wingtur=.455/(log10(Rey_wing_crs))^2.58;
Cf_wing_crs=.35*Cf_winglam+.65*Cf_wingtur;
Cf_winglam=1.328/sqrt(Rey_wing_TO);
Cf_wingtur=.455/(log10(Rey_wing_TO))^2.58;
Cf_wing_TO=.35*Cf_winglam+.65*Cf_wingtur;

Cf_HTlam=1.328/sqrt(Rey_HT_crs);
Cf_HTtur=.455/(log10(Rey_HT_crs))^2.58;
Cf_HT_crs=.35*Cf_HTlam+.65*Cf_HTtur;
Cf_HTlam=1.328/sqrt(Rey_HT_TO);
Cf_HTtur=.455/(log10(Rey_HT_TO))^2.58;
Cf_HT_TO=.35*Cf_HTlam+.65*Cf_HTtur;

Cf_VTlam=1.328/sqrt(Rey_VT_crs);
Cf_VTtur=.455/(log10(Rey_VT_crs))^2.58;
Cf_VT_crs=.35*Cf_VTlam+.65*Cf_VTtur;
Cf_VTlam=1.328/sqrt(Rey_VT_TO);
Cf_VTtur=.455/(log10(Rey_VT_TO))^2.58;
Cf_VT_TO=.35*Cf_VTlam+.65*Cf_VTtur;

FF_wing=(1+.6/.3*.15+100*.15^4)*(1.34*M^.18*(cos(6*pi/180))^.28);
FF_tail=1.1*((1+.6/.3*.10+100*.10^4)*(1.34*M^.18*(cos(6*pi/180))^.28));
f_fuse=l_fuse/8;
f_nac=12/2.5;
FF_fuse=(1+60/f_fuse^3+f_fuse/400);
FF_nac=(1+60/f_nac^3+f_nac/400);

Q_nac=1.5;
```

```
Q_wing=1.1;
Q_HT=1.04;
Q_VT=1.04;

CD_0_upswp=3.83*(15*pi/180)^2.5*4.5^2*pi/S_ref;
CD_0_tire1=.25/(27*7.5);
CD_0_tire2=.15/(27*7.5);
CD_0_frttire1=.25/(19*5.3);
CD_0_frttire2=.15/(19*5.3);
CD_0_struts=.05/(.5*7);

CD_0crs=(((Cf_fuse_crs*FF_fuse*S_wetFuse+Cf_nacelle_crs*FF_nac*Q_nac*S_wetEng
+Cf_wing_crs*FF_wing*Q_wing*S_wetW+...

Cf_VT_crs*FF_tail*Q_VT*S_wetVT+Cf_HT_crs*FF_tail*Q_HT*S_wetHT)/(S_ref))+CD_0_
upswp)*1.1;
CD_0TO=(((Cf_fuse_crs*FF_fuse*S_wetFuse+Cf_nacelle_crs*FF_nac*Q_nac*S_wetEng+
Cf_wing_crs*FF_wing*Q_wing*S_wetW+...

Cf_VT_crs*FF_tail*Q_VT*S_wetVT+Cf_HT_crs*FF_tail*Q_HT*S_wetHT)/(S_ref))+CD_0_
upswp+CD_0_tire1*2+...
    CD_0_tire2*2+CD_0_frttire1+CD_0_frttire2+CD_0_struts)*1.1;

fprintf('Parasite Drag in Cruise: %.3f\n\n',CD_0crs)
fprintf('Parasite Drag in TO/Landing: %.3f\n\n',CD_0TO)

fprintf('============================================================\n\n')
fprintf('Center of Gravity\n\n\n')

wing_loc=35.3;
tail_loc=81;
CG_wing=W_wing*wing_loc;
CG_HT=W_HT*tail_loc;
CG_VT=W_VT*83.2;
CG_fuse=W_fuse*38;          % Center of Structure
CG_MLG=W_MLG*41.5;
CG_NLG=W_NLG*10.4;
CG_nac=W_nacelle*(wing_loc-6.1);
CG_engcon=W_engcon*(wing_loc-6.1);
CG_start=W_start*(wing_loc-6.1);
CG_fuelsys=W_fuelsys*37.9;
CG_flightcon=W_flightcon*38.9;      % Distributed amongst plane, point at
center
CG_APU=W_APU*70;
CG_instru=W_instru*9.5;
CG_hydro=W_hydro*42;    % Distributed amongst plane, point at center
CG_elec=W_elec*38;      % Distributed amongst plane, point at center
CG_avion=W_avion*7;
CG_furn=W_furn*19.8;
CG_AC=W_AC*55;
CG_antiice=W_antiice*40;
CG_engine=W_engine*(wing_loc-6.1);
CG_passseats=W_passseats*40;
CG_pilotseats=W_pilotseats*13.3;
```

```
CG_lavatory=W_lavatory*60;
CG_baggage=44*30*66.5;
CG_passengers=176*30*40;
CG_crew=W_crew*30;
CG_fuel=W_fuel*39;

CG_empty=(CG_wing+CG_HT+CG_VT+CG_fuse+CG_MLG+CG_NLG+CG_nac+CG_engcon+CG_start
+CG_fuelsys+CG_flightcon+CG_APU+CG_instru+CG_hydro+CG_elec+CG_avion+CG_furn+C
G_AC+CG_antiice+CG_engine+CG_passseats+CG_pilotseats+CG_lavatory)/W_empty;

CG_fullfuel=(CG_empty*W_empty+CG_fuel)/(W_empty+W_fuel);

CG_MTOW=(CG_empty*W_empty+CG_fuel+CG_crew+CG_passengers+CG_baggage)/W_0calc;

CG_passnofuel=(CG_empty*W_empty+CG_crew+CG_passengers+CG_baggage)/(W_empty+W_
payload+W_crew);

CG_crs=(CG_MTOW+CG_passnofuel)/2;

fprintf('Empty Center of Gravity: %.1f ft\n\n',CG_empty)
fprintf('Fuel Only Center of Gravity: %.1f ft\n\n',CG_fullfuel)
fprintf('Full Payload, Empty Fuel Center of Gravity: %.1f
ft\n\n',CG_passnofuel)
fprintf('MTOW Center of Gravity: %.1f ft\n\n',CG_MTOW)

%% Stability Calculations
% Declaration of variables followed by defining the major equations provided
in Ch. 16. The variables will
% then be filled in with each flight condition's respective values. The
equations will then be evaluated.

fprintf('============================================================\n\n')
fprintf('Longitudinal Stability Calculations\n\n\n')

% Defining the variables (cruise)

S_horz=S_horz*.9;
N_B=6;          % Double Check
A_p=143.1;          % Double Check
AR_h=4;         % Double Check
lambda_maxt_h=25*pi/180;    % Double Check
K_fus=.027;
lambda_maxt=2*pi/180;
parCl_parel=3.89;
parCl_parf=2.14;
X_acw=((wing_loc-.3*C_root)+x+C_bar*.25)/C_bar; % Double Check
X_ach=(tail_loc/C_bar);     % Double Check
X_p=(wing_loc-8.6)/C_bar;
eta_h=.9;
diam=9.1;
W_f=diam;

for k=0:1:2
```

```
    if (k==0)
    approach_Factor=1.0;
    parep_u_para=.9;
    Mach=.358;
    Beta=sqrt(1-Mach^2);
    C_l_a=2*pi;
    q=.5*V_fts^2*rho_cruise;
    parCNblade_para=.125;
    parep_para=.25;
    K_1=.14;
    K_2=.25;
    f_T=1.2;
    gear_moment=0;
    fprintf('Cruise Conditions\n\n')
    end

    if (k==1)
    % Defining the variables (TO)

    approach_Factor=1.0;
    parep_u_para=.9;
    Mach=.106;
    K_f=.65;
    S_el=S_horz*.3;
    parCl_parf=3.75;
    Delta_fl=pi/6;
    Delta_el=pi/12;
    lambda_HL_W=-pi/36;
    lambda_HL_HT=-pi/36;
    Beta=sqrt(1-Mach^2);
    C_l_a=4.882;        % XFoil
    q=.5*(1.15*.8*V_stall)^2*rho_SL;
    parCNblade_para=.082;       % Double Check
    parep_para=.25;     % Double Check
    K_1=.36;            % Double Check
    K_2=.23;            % Double Check
    f_T=1.55;           % Double Check
    gear_moment=((CG_MTOW-44.7)*(W_empty+W_payload+W_crew-
C_L_TO*q*S_ref)+.03*8*(W_empty+W_payload+W_crew-
C_L_TO*q*S_ref))/(q*S_ref*C_bar);
    fprintf('\nTakeoff Conditions\n\n')
    end

    if (k==2)
    % Defining the variables (Approach)

    approach_Factor=1.1;
    parep_u_para=.45;
    Mach=.15;
    K_f=.65;
    S_el=S_horz*.3;
    parCl_parf=3.75;
    Delta_fl=pi/6;
```

```
    Delta_el=pi/12;
    lambda_HL_W=-pi/36;
    lambda_HL_HT=-pi/36;
    Beta=sqrt(1-Mach^2);
    lambda_maxt=2*pi/180;
    C_l_a=4.882;        % XFoil
    q=.5*(1.3*V_stall)^2*rho_SL;
    parCNblade_para=.082;       % Double Check
    parep_para=.25;     % Double Check
    K_1=.36;            % Double Check
    K_2=.23;            % Double Check
    f_T=1.55;           % Double Check
    gear_moment=0;
    fprintf('\nApproach Conditions\n\n')
    end
% Defining Equations

F=1.07*(1+diam/b);
Beta=sqrt(1-Mach^2);
eta=C_l_a/(2*pi/Beta);
C_L_a=((2*pi*AR)/(2+sqrt(4+(AR^2*Beta^2/eta^2)*(1+(tan(lambda_maxt))^2/Beta^2
)))*S_expW/S_ref*F)*approach_Factor;
C_L_a_h=((2*pi*AR_h)/(2+sqrt(4+(AR_h^2*Beta^2/eta^2)*(1+(tan(lambda_maxt_h))^
2/Beta^2)))*S_horz*.8/S_horz*F)*approach_Factor;
C_m_afus=K_fus*W_f^2*l_fuse/(C_bar*S_ref)*180/pi;
para_p_para=1+parep_u_para;
parep_p_para=K_1+K_2*N_B*parCNblade_para*para_p_para;
para_h_para=1-parep_para-parep_p_para;
F_P_a=q*N_B*A_p*parCNblade_para*f_T;
X_np=(C_L_a*X_acw-
C_m_afus+eta_h*S_horz/S_ref*C_L_a_h*para_h_para*X_ach+F_P_a/(q*S_ref)*para_p_
para*X_p)/(C_L_a+eta_h*S_horz/S_ref*C_L_a_h*para_h_para+F_P_a/(q*S_ref))+gear
_moment;

if(k==0)
C_L_a_crs=C_L_a;
C_L_a_h_crs=C_L_a_h;
C_m_afus_crs=C_m_afus;
F_P_a_crs=F_P_a;
q_crs=q;
end

fprintf('Neutral Point location on MAC: %.1f ft\n\n',X_np)
fprintf('Neutral Point location from Nose: %.1f ft\n\n',X_np*C_bar)
fprintf('MTOW Static Margin: %.1f percent\n\n',((X_np*C_bar)-
CG_MTOW)/C_bar*100)
fprintf('No Passengers Static Margin: %.1f percent\n\n',((X_np*C_bar)-
CG_fullfuel)/C_bar*100)
    if(k!=1)
    fprintf('Empty Fuel Static Margin: %.1f percent\n\n',((X_np*C_bar)-
CG_passnofuel)/C_bar*100)
    end
end
```

```
%% Trim Calculations

k=1;
h=1;
S_el=S_horz*.4;
for(Delta_el=-pi/90:pi/90:pi/90);
for(alpha=0:pi/180:pi/18);
K_el=1;
parCL_parel=.9*K_el*(parCl_parel)*S_el/S_horz*cos(lambda_HL_HT);
del_a_0Lel=((-1/C_L_a_h)*parCL_parel)*Delta_el;
C_m_0airfoil=-.1041;
i_w=0;
i_h=-pi/30;
alpha_0L=-4.2*pi/180;
C_m_W_delf=0;
Z_t=0;

C_m_W=C_m_0airfoil*(AR*(cos(lambda_maxt))^2/(AR+2*cos(lambda_maxt)));
C_L=C_L_a_crs*(alpha+i_w-alpha_0L);
C_m_fus=C_m_afus_crs*alpha;
C_L_h=C_L_a_h_crs*((alpha+i_w)*(1-parep_para)+(i_h-i_w)-del_a_0Lel);
F_P=F_P_a_crs*alpha;

C_L_total(k,h)=C_L_a_crs*(alpha+i_w)+eta_h*S_horz/S_ref*C_L_h;

C_m_CG(k,h)=C_L*(CG_crs/C_bar-X_acw)+C_m_W+C_m_W_delf*Delta_fl+C_m_fus-
eta_h*S_horz/S_ref*C_L_h*(X_ach-CG_crs/C_bar)-
T_W0_crs_match*W_0calc*.95/(q_crs*S_ref)*Z_t+F_P/(q_crs*S_ref)*(CG_crs/C_bar-
X_p);

h=h+1;
end
k=k+1;
end

figure
scatter(C_L_total,C_m_CG),axis([-.1,1,-.1,.1])
hold on
x=-1:.01:2;
y=0*x;
scatter(x,y)
hold off

%% Lateral Stability

fprintf('============================================================\n\n')
fprintf('Lateral Stability Calculations\n\n\n')

AR_v=2;
VT_sweep=pi/3;
Z_wf=22.25; % Height of VT above centerline
D_f=9.1;        % Depth of fuselage
W_fuse=8;       % Width of fuselage
```

```
tau=pi/180;      % Wing dihedral
Z_barv=13.5;     % Distance to VT MAC vertically from CG
taper_VT=.25;
C_l_B_wing_C_L=-.22;     % Fig 16.21
volume=625; % get from model
Thrust=T_W_OEI*W_0calc/2;
Y_p=14.3;        % get from model
parCNblade_parB=parCNblade_para;
K_rvt=.95;
parCf_pardelru=3.5;
lambda_HL_VT=10*pi/180;
i_v=0;
sidewash=0; % Negligible due to lack of fuselage influence and prop wash
S_vert=S_vert*.9;
S_rud=.3*S_vert;

for(h=0:1:20)
Delta_ru=-h*pi/180;

for(k=0:1:1)
if(k==0)         %Takeoff OEI
V=V_stall*1.15;
M=V/587;
Beta=sqrt(1-M^2);
q=.5*rho_SL*V^2;
Beta_vert=0*pi/180;
end
if(k==1)         %Landing Crosswind
V=V_stall*1.3;
M=V/587;
Beta=sqrt(1-M^2);
q=.5*rho_SL*V^2;
Beta_vert=11.5*pi/180;
end

D_p=(.1*sigma*pi*(13.5/2)^2)*q; % Eq. 12.39
C_n_B_w=(C_L_a_crs*pi/90)^2*(1/(4*pi*AR_v)-
(tan(VT_sweep)/(pi*AR_v*(AR_v+4*cos(VT_sweep))))*(cos(VT_sweep)-AR_v/2-
AR_v^2/(8*cos(VT_sweep))+6*(X_acw-CG_crs/C_bar)*sin(VT_sweep)/AR_v));
C_n_B_fus=-1.3*volume/(S_ref*b)*D_f/W_fuse;
parB_v_parB_eta_v=.724+3.06*(S_vert/S_ref)/(1+cos(VT_sweep))-
.4*Z_wf/D_f+.009*AR_notips;
F=1.07*(1+D_f/Z_wf);
C_F_B_v=2*pi*AR_v/(2+sqrt(4+AR_v^2*Beta^2/eta^2*(1+(tan(VT_sweep))^2/Beta^2))
)*.95*F;
C_n_B_v=C_F_B_v*parB_v_parB_eta_v*S_vert/S_ref*(tail_loc-CG_crs/C_bar);
F_P_B=q*N_B*A_p*parCNblade_parB*f_T;

C_l_B_wf=-1.2*sqrt(AR_v)*Z_wf*(D_f+W_fuse)/b^2;
C_l_B_tau=-C_L_a_crs*tau/4*(2/3*(1+2*taper_VT)/(1+taper_VT));
C_l_B_w=C_l_B_wing_C_L*C_L_a_crs*pi/90+C_l_B_tau+C_l_B_wf;
C_l_B_v=-C_F_B_v*parB_v_parB_eta_v*S_vert/S_ref*Z_barv;

parCF_parru=.9*K_rvt*parCf_pardelru*S_rud/S_vert*cos(lambda_HL_VT);
```

```
del_B_0Lru=(-1/C_F_B_v)*parCF_parru*Delta_ru;
Beta_v=(Beta_vert+i_v)*(1-sidewash)+i_v-del_B_0Lru;

C_l=C_l_B_w*Beta_vert+C_l_B_v*Beta_vert;

C_n_B=C_n_B_w+C_n_B_fus+C_n_B_v-2*F_P_B/(q*S_ref)*para_p_para*CG_MTOW/(C_bar-
X_p);
if(k==0)
C_n=C_n_B_w*Beta_vert+C_n_B_fus*Beta_vert+C_n_B_v*Beta_v-
(F_P_B*Beta_vert*(CG_crs/C_bar-X_p)+.5*Thrust*Y_p+D_p*Y_p)/(q*S_ref);
end
if(k==1)
C_n=C_n_B_w*Beta_vert+C_n_B_fus*Beta_vert+C_n_B_v*Beta_v-
2*(F_P_B*Beta_vert*(CG_crs/C_bar-X_p))/(q*S_ref)
end
end
end
```

Performance, Gear Sizing, Propeller

```
% Description:Calculation of the performance parameters, tire sizing,
%              propeller sizing, strut sizing and oleo sizing code.
%Group 3
%Brian Omondi, Jacob Maynard, Adam Houtman.

ALT0=0.000
ALT=25000
W0=34202    %Gross weight in lbs
We=21749    %Empty weight in lbs
W_crs=31547.32  %Average weight at cruise in lbs
Wini=33175.94 %Initial weight at cruise
Wfin=29918.7
S=1005.5 %wing reference area in ft^2
CD0=0.0255
K=0.0376
eta_crs=0.8
eta_ploit=0.7
C_crs_bhp=0.5
C_loit_bhp=0.6
rho=0.002377   %density at sea level in slug/ft^3
rho_crs=10.663E-4
V=(0:10:300)*1.687809  %velocity in ft/sec
PA0=5880

V_stall=130*1.68781 %Defines the stall speed in ft/sec
P_W0=0.177  %Defines the power to weight ratio in hp/lb
V_crsknots=220;         % [knots]
V_crs=V_crsknots*1.688 %defines the velocity in ft/s

X=tsa(ALT,'eng');
RHO=X(3)
```

```
X=tsa(ALT0,'eng')
RHO0=X(3)
Vinf=30:15:1500

%PA and PR at Cruise
for i=1:length(Vinf)
    CL(i)=W_crs/(0.5*RHO*Vinf(i)^2*S);
    CD(i)=CD0+(K*CL(i)^2);
    D(i)=CD(i)*0.5*RHO*Vinf(i)^2*S;
    TR(i)=D(i)
    PR(i)=TR(i)*Vinf(i)
    PR_hp(i)=PR(i)/550;
    PA(i)=PA0*((RHO/RHO0)^0.7);
    PA_hp(i)=eta_crs*PA(i)
    TA=eta_crs*PA(i)./Vinf

end

V_crsknots=220;         % [knots]
V_crs=V_crsknots*1.688 %defines the velocity in ft/s


figure(1)
plot(Vinf*0.592484,PR_hp,Vinf*0.592484,PA_hp)
title(['PR vs PA for Sonata:
W=',num2str(W_crs),'lbs','ALT=',num2str(ALT),'ft'])
xlabel('Velocity,knots'),ylabel('power, hp'),grid
legend('Power required (PR)','Power Available (PA)')

%Coefficient of Lift at cruise-25000 ft
CL_crs=W_crs/(0.5*rho_crs*(V_crs)^2*S)


%Calculation of maximum L/D and maximum (CL^(3/2)/CD)
LDmax=sqrt(1/(4*CD0*K))
CL32CDmax=(1/4)*(3/(K*(CD0)^(1/3)))^(3/4)

%Calculation of maximum range and endurance velocities
VLDmax=sqrt((2/rho_crs)*sqrt(K/(CD0))*W_crs/S) %Velocity in ft/sec
VCL32CDmax=sqrt((2/rho_crs)*sqrt(K/(3*CD0))*W_crs/S) %Velocity in
ft/sec

%Specific fuel consumption unit conversions
C_range=0.5/(550*3600)   %Units of 1/ft
C_loit=0.6/(550*3600)    %units of 1/ft

%Maximum range and Endurance calculations
R_max=(eta_crs/C_range)*LDmax*log(32082/29267)
Rmax=R_max/6076.12  %Defines the maximum range in nautical miles
```

```
E_max=(eta_ploit*CL32CDmax/(C_loit*1.4*V_stall))*log(32082/29267)
Emax=E_max/3600  %Maximum endurance in hours

%Min. sink rate and airspeed,maximum glide range and airspeed
calculations
theta_min=atan(1/(LDmax)) %minimum glide angle in radians
theta_mindegree=(theta_min/(2*pi))*360  %minimum glide angle in
degrees
Sink_min=sqrt(2/(rho_cruise*CL32CDmax)*(W_crs/S));  %minumum sink rate
in ft/sec.
Sink_minvel=VCL32CDmax  %minimum sink velocity in ft/sec
GlideR_max=25000/(LDmax*5280)  %maximum glide range in miles at 25000
ft
GlideR_maxvel=VLDmax    %velocity for maximum glide range in ft/sec

%Maximum Rate of Climb and Velocity for maximum Rate of Climb
V_ROCmax=sqrt(2/rho_cruise*sqrt(K/(3*CD0))*W_crs/S)  %Defines the
velocity for maximum rate of climb in ft/s
ROCmax=(eta_crs*P_W0)*550-(V_ROCmax*1.155/(LDmax))   %Defines the
maximum rate of climb in ft/s

%Power Loading at absolute ceiling
rho_ceil=(2*(W_crs/S)*sqrt(K/(3*CD0)))/(eta_crs*550*P*LDmax/(W_crs*1.1
55))^2
Rho_ceil=2*(W_crs/S)*sqrt(K*(3*CD0))/...
  ((eta_crs*P*550/W_crs)-(1.667*LDmax)/1.155)^2
%For the density of 0.0009 slug/ft^3 ,the...
%ceiling at 100 ft/min the altitude is approximately 28000 ft

%Propeller Calculations in SI units
%From Aircraft design book by Mohamed Sadraey
ARp=7   %Defines the propeller aspect ratio,typically between 8-14
V_tip=250    %Tip speed limits in m/sec
V_av=0.7*V_tip %Average speed of the propeller in m/s
CLp=0.4  %Typically between 0.2-0.4
rho_crsSI=0.54939382  %cruise density in kg/m^3
P=5880  %Total power available in hp
Dp=0.72*sqrt(2*(PA0/2)*eta_crs*745.699872*ARp/(rho_crsSI*(V_av^2)*CLp*
V_crsknots*0.514))...
    %A 6 blade will be used as a propeller with a smaller no .of
blades
    %will necessitate the use of a very long propeller which will also
have
    %problems such as tip speed exceeding speed of sound
% Propeller rotational speed
Dp_ft=(Dp*39.3701)/12
Vtip_static=sqrt(V_tip^2-(V_crsknots*0.514)^2)
omega_prop=(2*Vtip_static/Dp)*(60/(2*pi))  %Engine shaft speed in
rev/min
```

```
%From engine data the P&W engine has a ratational shaft speed of 1200
rpm
%therefore a gearbox might be used to reduce the speed to 1200 rpm
n_s=1200            %Engine shaft rotational speed
GR=omega_prop/n_s   %Gear box ratio to prevent the shaft from
exceeding the speed required

%Tire sizing
%Raymer Table 11.1
Ww=((0.9)*W0/4)  %Weight in each main wheel in lbs
A_d=1.63
B_d=0.315
D=A_d*Ww^B_d   %Main wheel diameter in inches
A_w=0.1043
B_w=0.480
w=A_w*Ww^B_w   %Main wheel width in inches
W_nw=((0.1)*W0/2)
A_dn=1.63
B_dn=0.315
D_n=A_dn*W_nw^B_dn   %Nose wheel diameter in inches
A_wn=0.1043
B_wn=0.480
w_n=A_wn*W_nw^B_wn   %Nose wheel width in inches
H_clr=9/12  %propeller ground clearance
H_cg=(H_clr+Dp_ft/2)/12 % Distance from the ground to c.g of plane in
ft
B=31.1  %Distance from the main gear to the nose gear
M_f=5.5  %Distance from the forward c.g to the main gear
N_f=B-M_f   %Distance between the forward c.g and the nose gear
N_a=28.3  %Distance from the nose gear to the aft c.g
M_a=B-N_a  %Distance between the aft c.g and the main gear
%N_b=28.6   %Distance from the nose gear to the aft c.g
Stac_max=W0*(N_a/B)  %Maximum static load of the main gear
Stac_maxper=Stac_max/4  %Maximum static load in each main gear
Stat_min=W0*(N_f/B)   % minimum static load of the main gear
Stat_minper=Stat_min/4  %Minimum static load in each main gear
Stat_max_nose=(W0*M_f)/B  %Maximum static load in the nose gear in lbs
Stat_max_pern=Stat_max_nose/2  %Maximum static nose load per gear in
lbs
Stat_min_nose=W0*M_a/B    %Minimum static load in the nose gear in lbs
Stat_min_pern=Stat_min_nose/2  %Minimum static load of the nose per
gear in lbs
g=32.2  %Gravity in ft/sec^2
Brak_load_dyn=10*W0*H_cg/(g*B)   %Dynamic braking Load


%Using Raymer's Textbook in calculation of Static loads on the
tires...
%we need to add a 7% margin should be added to all calculated wheel
loads.
```

```
%Also it is common to add 25% of the total loads for later growth of
the
%aircraft design
%7% and 25% margin added for future growth
Stac_max=(W0*(N_a/B)*1.07)*1.25  %Maximum static load of the main gear
Stac_maxper=Stac_max/4  %Maximum static load in each main gear
Stat_min=W0*(M_a/B)*1.07*1.25   % minimum static load of the main gear
Stat_minper=Stat_min/4 %Minimum static load in each main gear
Stat_max_nose=(W0*M_f)/B*1.07*1.25  %Maximum static load in the nose
gear in lbs
Stat_max_pern=Stat_max_nose/2  %Maximum static nose load per gear in
lbs
Stat_min_nose=W0*M_a/B*1.07*1.25    %Minimum static load in the nose
gear in lbs
Stat_min_pern=Stat_min_nose/2  %Minimum static load of the nose per
gear in lbs

%Maximum load on the nose and main gear
Load_max_nose=(W0*M_f)/B+(W0*10*H_cg)/(g*B)   %Maximum nose gear load
which...
                              %is achieved during landing braking
Load_max=((W0*N_a)/B)+(W0*4*3.2808399*H_cg)/(g*B)  %Maximum main
gear...
        %load which is achieved during takeoff acceleration assuming
an...
        %acceleration of 4 m/s^2 which is converted to  english units
for
        %consistency
Load_max_pern=Load_max_nose/2  %Maximum load in each nose gear in lbs
Load_maxperm=Load_max/4  %maximum load in each main gear in lbs
KE_braking=0.5*W0*V_stall^2/32.2  %braking kinetic energy
N_gear=3
N_ult=1.3*N_gear  %Ultimate load factor fot structural safety
considerations
V_vert=10  %Defines the vertical speed in ft/sec
eta=0.75  %Oleopneumatic metered orifice efficiency
eta_t=0.47  % efficiency of the tire
S_T=11.85  %Defines tire radius as specified by raymer as
%two thirds of tire diameter
%Stoke calculations
S=V_vert^2/(2*g*eta*N_gear)-(eta_t/eta)*S_T
Oleo_load=Stac_max/2 %Oleo load for the main gear
Oleo_loadn=Load_max_nose  %Oleo load for main gear which is equal
%to total maximum load on the nose gear
pressure_int=1800  % Defines the pressure in psi
mainD_oleo=1.3*sqrt((4*Oleo_load)/(pressure_int*pi)) %Main gear oleo
diameter
noseD_oleo=1.3*sqrt((4*Oleo_loadn)/(pressure_int*pi))  %Nose gear oleo
diameter
```

```
rR_main_g=(2/2.3)*(D/2)   %Defines the approximation of tire rolling
radius
%in inches as prescribed by Raymer

Ap=2.3*sqrt(w*D)*(D/2-rR_main_g)  %Pavement area for main tire in in^2
Ap_n=2.3*sqrt(w_n*D_n)*(D_n/2-7.9)    %Pavement area for the nose tire
in in^2
P=70  %Maximum pressure assuming the airplane will work ar place with
tarmac
%with a good foundation as is in most regional airports
W_tire=P*Ap  %Weight carried by the tire in lbs
W_tire_nose=P*Ap_n %Weight carried by the nose wheel tire in lbs

%Landing gear design
C_bar=8.7606*12  %Mean aerodynamic center in in
Dp_in=Dp*39.3701
H_clr=9  %propeller ground clearance
H_cg=(H_clr+Dp_in/2)/12 % Distance from the ground to c.g of plane
t_cmax=0.15  %From the airoil NACA 4415
tw=t_cmax*C_bar  %wing thickness in inches
H_LG=H_cg-tw/2   %Landing gear height in inches is chosen to ensure
that there is a 7...
%inch clearance between the propeller and the ground-FAR25 regulations
%The main gear attachment will be finalized once the wheel base and
wheel
%wheel track have been determined
```

Cost Analysis

```
%% Sonata cost analysis

We=21552 % Empty weight in lbs
Wavionics=1235 % Weight of avionics
V=220:5:325 % Maximum velocity in kts
Q=200 % Production quantity
FTA=2 % Number of flight test airframes
Vc=210 % Cruise velocity
Wo=34202 % Takeoff gross weight
Np=35 % Number of passengers

HE=5.18*(We^.777)*(V.^.894)*(Q^.163) % Engine hours Eqn 18.1
HT=5.99*(We^.777)*(V.^.696)*(Q^.263) % Tooling hours Eqn 18.2
HM=1.1*(7.37*(We^.82)*(V.^.484)*(Q^.641)) % Manufacturing hours Eqn 18.3
HQ=.133*HM % Quality control hours Eqn 18.4
CD=91.3*(We^.63)*(V.^1.3) % Development Support Cost Eqn 18.5
CF=2498*(We^.325)*(V.^.822)*(FTA^1.21) % Flight test costs Eqn 18.6
CM=22.1*(We^.921)*(V.^.621)*(Q^.799) % Manufacturing materials cost Eqn 18.7
PassC=1700*Np % Cost added; $1700 per passenger

% Engine production costs
Ceng=2000000
Ne=2*Q % Total Number of engines for production
```

```
Ne_AC=2 % Number of engines per aircraft

Cavionics=Wavionics*5000 %Avioncis cost with $6k per pound of avionics

% Rates
RE=115 % Engineering rate
RT=118 % Tooling
RQ=108 % Quality control
RM=98 % Manufacturing

% RDT & E and flyaway costs
RDTE_FC=HE*RE+HT*RT+HM*RM+HQ*RQ+CD+CF+CM+Ceng*Ne+Cavionics % Eqn 18.9

% Cost per aircraft
C_A=(RDTE_FC/Q)+(PassC)

% Fuel costs
FH_YR_AC=3000 % Flight hrs/yr/aircraft est from Table 18.1
JetA=6.39 % Jet A prices at KBTL per gal
TBR=205 % Typical mission profile fuel burn rate
FuelCosts=JetA*TBR*FH_YR_AC % Total fuel costs

% Block hours
FR=700 % Normal flight range in NM
BD=(1+((.015+(7/FR))*100)*FR) % Block distance
FT=2 % Estimated flight time in hrs
BT=FT+.35 % Estimated block time in hrs
BV= BD/BT % Estimated block velocity
BH_YR=BT/FT*FH_YR_AC % Estimated Block time per year

% Crew salaries
TwoCS=70.4*(Vc*(Wo/(10^5)))^.3+168.8 % 2 man crew Eqn 18.10
ThreeCS=94.5*(Vc*(Wo/(10^5)))^.3+237.2 % 3 man crew Eqn 18.11
TwoCS_yr=TwoCS*BH_YR % 2 crew yearly pay
ThreeCS_yr=ThreeCS*BH_YR % 3 crew yearly pay

% Maintenance Expenses
% Maintenance Man hrs/flight hr
MMH_FH=5
% Cost of aircraft minus engines
CA=C_A-(Ceng*Ne_AC)
% Material costs per flight hour Eqn 18.12
MC_FH=3.3*(CA/(10^6))+14.2+(58*(Ceng/(10^6))-26.1)*Ne_AC
% Material cost per cycle Eqn 18.13
MC_cycle=4*(CA/(10^6))+9.3+(7.5*(Ceng/(10^6))+5.6)*Ne_AC
% Maintenance Man hrs/hr
MMH_YR=MMH_FH*FH_YR_AC
% Material costs per year from flight hrs
MC_Flight=MC_FH*FH_YR_AC
% Number of cycles
NumC=BH_YR/BT
% Material costs per year from cycles
MC_Cyc=MC_cycle*NumC
```

```
% Total material costs
MC_Total=MC_Flight+MC_Cyc

figure
plot(V, C_A), xlabel('Max speed in knots'), ylabel('Aircraft cost in $')

figure
plot(V, MC_Total), xlabel('Max speed in knots'), ylabel('Total Material cost
in $')
```

APPENDIX C) Drawing Package

NOTE: Dimensions may not match those used in calculations! Check reference points of dimensions in drawings when comparing too those used in calculations.

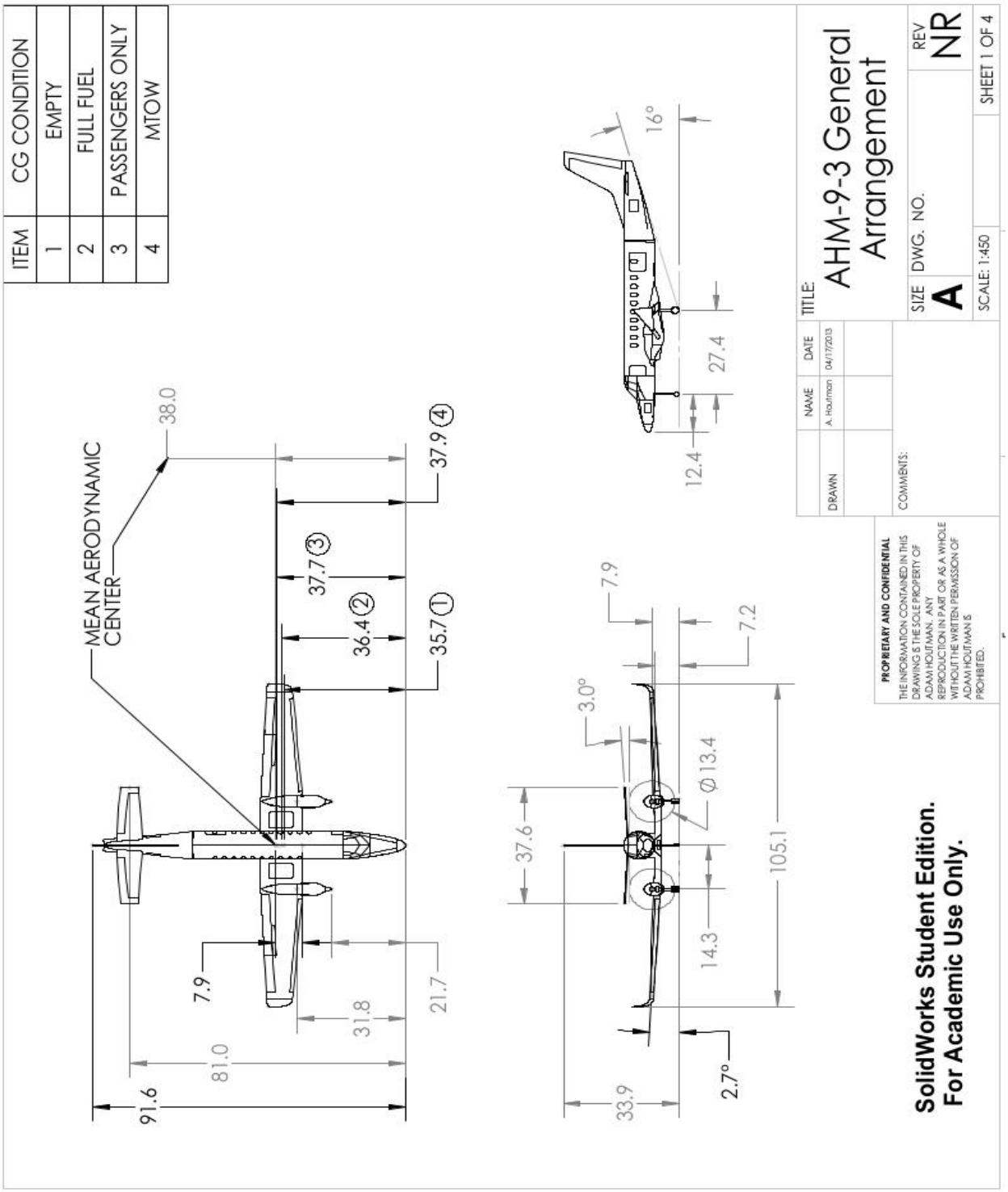

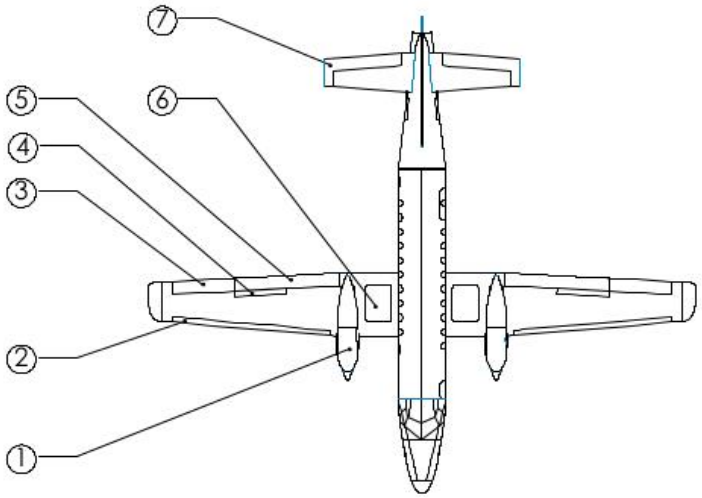

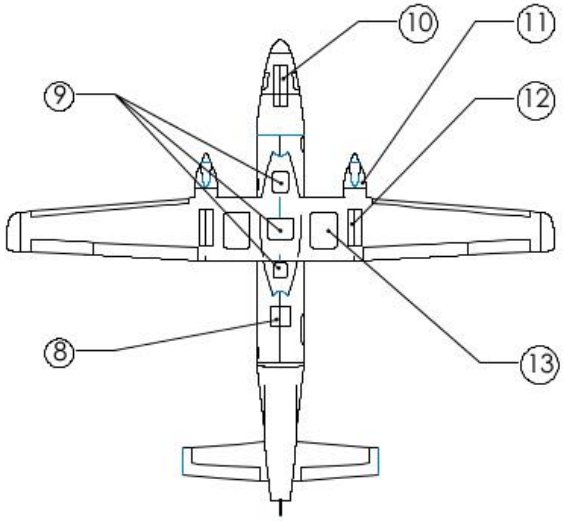

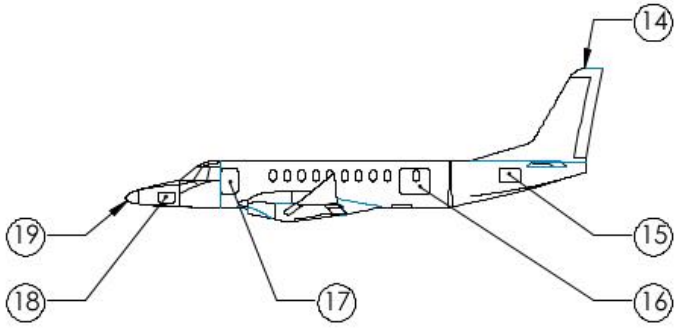

19	WEATHER RADAR
18	AVIONICS ACCESS
17	MAIN PASSENGER DOOR
16	CARGO DOOR
15	SIDE ACCESS APU
14	RUDDER WITH MASS BALANCE
13	FUEL TANK ACCESS
12	MAIN GEAR DOOR
11	LOWER FORWARD COWL
10	NOSE GEAR DOOR
9	BELLY ACCESS
8	REAR BELLY ACCESS
7	ELEVATOR WITH MASS BALANCE
6	FUEL TANK ACCESS
5	FLAP
4	SPOILER
3	AILERON
2	LEADING EDGE SLAT
1	UPPER ENGINE COWL

	NAME	DATE
DRAWN	A. Houtman	04/17/2013

COMMENTS:

TITLE:
AHM-9-3 General Arrangement

SIZE	DWG. NO.	REV
A		NR

SCALE: 1:350 SHEET 2 OF 5

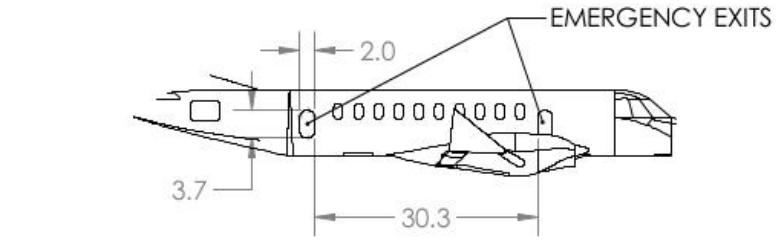

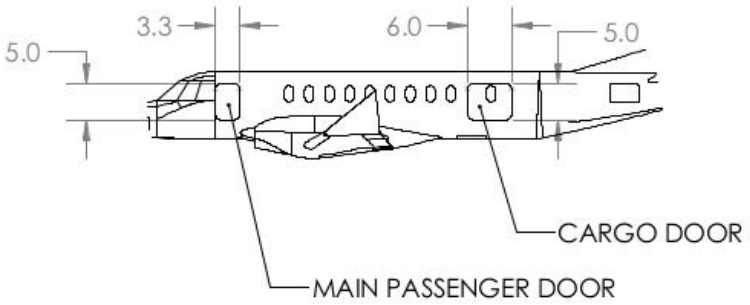

	NAME	DATE
DRAWN	A. Houtman	04/17/2013
COMMENTS:		

TITLE: AHM-9-3 General Arrangement

SIZE	DWG. NO.	REV
A		NR

SCALE: 1:250 SHEET 3 OF 5

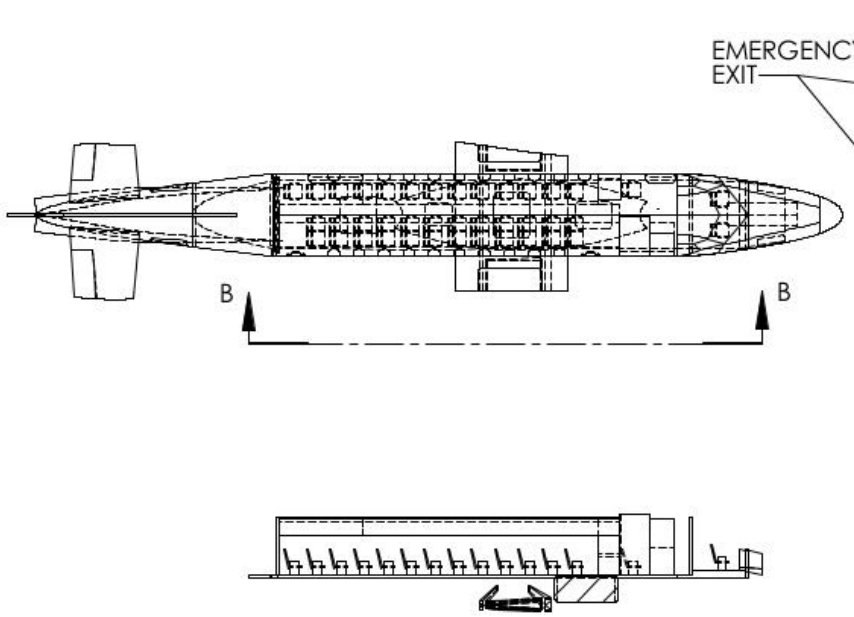

SECTION B-B

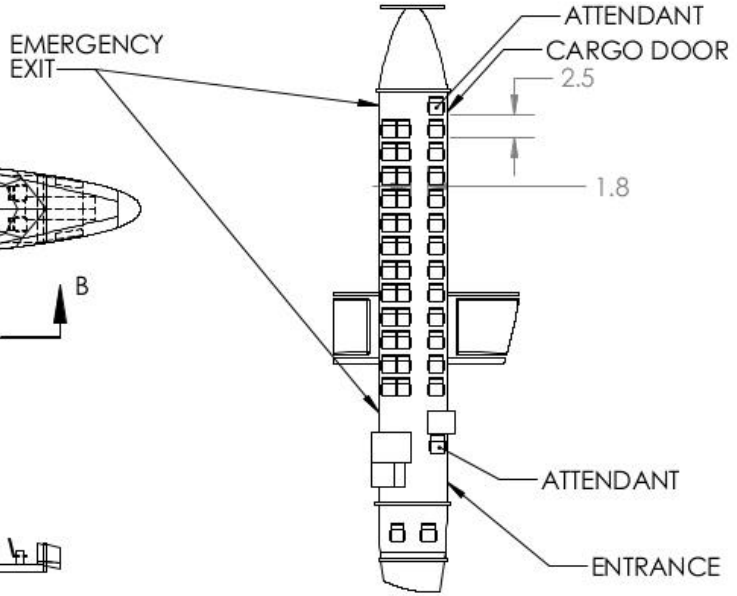

	NAME	DATE
DRAWN	A. Houtman	04/17/2013

TITLE:

AHM-9-3 General Arrangement

SIZE	DWG. NO.	REV
A		

SCALE: 1:200 SHEET 4 OF 5

COMMENTS:

Works Cited

"Beechcraft 1900." 2012. *Airlines Inform.* http://www.airlines-inform.com/commercial-aircraft/Beech-1900.html. February 2013.

"Bombardier Dash 8-100/200." 2012. *Airlines Inform.* http://www.airlines-inform.com/commercial-aircraft/Dash-8Q200.html. February 2013.

"EMB120 Brasilia." n.d. *Airliners.net.* http://www.airliners.net/aircraft-data/. February 2013.

"Hamilton Standard Hydromatic Propeller." n.d. *Napolean130.* http://napoleon130.tripod.com/id697.html. February 2013.

Meier, Nathan. "Turboprop Specifications." 21 Mar 2005. *jet-engine.net.* http://www.jet-engine.net/miltsspec.html. February 2013.

"PW120." n.d. *Pratt and Whitney Canada.* http://www.pwc.ca/en/engines/pw120. February 2013.

Raymer, Daniel P. *Aircraft Design: A Conceptual Approach Fifth Edition*. Reston: AIAA, 2012.

"Saab 340." 2012. *Airlines Inform.* http://www.airlines-inform.com/commercial-aircraft/SAAB-340.html. February 2013.

Sadraey, Mohammed H. *Aircraft Design*. West Sussex: Wiley, 2013. Book.

"US Standard Atmosphere." n.d. *Engineering Toolbox.* http://www.engineeringtoolbox.com/standard-atmosphere-d_604.html. February 2013.

http://goodyearaviation.com/resources/pdf/datatires.pdf

http://www.flightsimbooks.com/flightsimhandbook/CHAPTER_02_10_Retractable_Landing_Gear.php